Clays and Clay Minerals, Vol. 61, No. 1, 34–56, 2013.

WEATHERING OF ALMANDINE GARNET: INFLUENCE OF SECONDARY MINERALS ON THE RATE-DETERMINING STEP, AND IMPLICATIONS FOR REGOLITH-SCALE Al MOBILIZATION

JASON R. PRICE[1,*], DEBRA S. BRYAN-RICKETTS[2,3], DIANE ANDERSON[1,4], AND MICHAEL A. VELBEL[2]

[1] Department of Earth Sciences, P.O. Box 1002, Millersville University, Millersville, PA 17551-0302, USA
[2] Department of Geological Sciences, 206 Natural Science Building, Michigan State University, East Lansing, Michigan 48824-1115, USA
[3] Environmental Protection Division, Los Alamos National Laboratory, Box 1663, Los Alamos, NM 87544, USA
[4] Celerity, 4720 Gettysburg Rd., Suite 204, Mechanicsburg, PA 17055, USA

Abstract—Secondary surface layers form by replacement of almandine garnet during chemical weathering. This study tested the hypothesis that the kinetic role of almandine's weathering products, and the consequent relationships of primary-mineral surface texture and specific assemblages of secondary minerals, both vary with the solid-solution-controlled variations in Fe and Al contents of the specific almandine experiencing weathering.

Surface layers are protective (PSL) when the volume of the products formed by replacement is greater than or equal to the volume of the reactants replaced. Under such circumstances, reaction kinetics at the interface between the garnet and the replacing mineral are transport controlled and either transport of solvents or other reactants to, or products from, the dissolving mineral is rate limiting. Beneath PSLs, almandine garnet surfaces are smooth, rounded, and featureless. Surface layers are unprotective (USL) when the volume of the products formed by replacement is less than the volume of the reactants replaced. Under such circumstances, reaction kinetics at the interface between the garnet and the replacing mineral are interface controlled and the detachment of ions or molecules from the mineral surface is rate limiting. Almandine garnet surfaces beneath USLs exhibit crystallographically oriented etch pits. However, contrary to expectations, etch pits occur on almandine garnet grains beneath some layers consisting of mineral assemblages consistent with PSLs.

Based on the Pilling-Bedworth criterion, surface layers are more likely to be protective over a broad range of reactant-mineral compositions when they contain goethite, kaolinite, and pyrolusite. However, this combination requires specific ranges of Fe and Al content of the natural reacting almandine garnet. To form a PSL of goethite and kaolinite, an almandine garnet must have a minimum Al stoichiometric coefficient of ~3.75 a.p.f.u., and a minimum Fe stoichiometric coefficient of ~2.7 a.p.f.u.

Product minerals also influence the mobility of the least-mobile major rock-forming elements. A PSL consisting of goethite, gibbsite, and kaolinite yields excess Al for export during almandine garnet weathering. As the quantity of kaolinite present in the PSL decreases, the amounts of Al available for export increases.

Key Words—Almandine Garnet, Chemical Weathering, Coweeta Hydrologic Laboratory, Gibbsite, Goethite, Hematite, Kaolinite, Protective Surface Layers, Saprolite, Unprotective Surface Layers.

INTRODUCTION

Weathering products are widely believed to exert an influence on the rates and mechanisms of primary-mineral weathering (Berner, 1978, 1981; Velbel, 1984a, 1993). However, specific examples of relationships between individual product minerals and distinctive alteration textures indicative of particular weathering mechanisms are not common. This is especially true when different weathering products are associated with different alteration textures. For example, denticulated (sawtooth, hacksaw, or 'cockscomb') terminations on naturally weathered pyroxenes and amphiboles appear identical regardless of whether the weathering product being formed is a 2:1 clay or an assemblage of hydroxides (*e.g.* Velbel, 1989, 2007; Velbel and Barker, 2008; Velbel *et al.*, 2009). These same textures also occur regardless of whether the environment of alteration is pedogenic or burial diagenetic (*e.g.* Berner *et al.*, 1980; Velbel, 2007).

Previous workers have reported almandine garnet weathering to various products, including gibbsite, goethite, and hematite (Embrechts and Stoops, 1982; Parisot *et al.*, 1983; Velbel, 1984a; Graham *et al.*, 1989a,b; Robertson and Butt, 1997). Additional studies have reported a great variety of garnet surface textures on both naturally weathered (Embrechts and Stoops, 1982; Parisot *et al.*, 1983; Velbel, 1984a, Ghabru *et al.*, 1989; Robertson and Butt, 1997) and diagenetically altered (Hansley, 1987; Salvino and Velbel, 1989) grains.

* E-mail address of corresponding author:
Jason.Price@millersville.edu
DOI: 10.1346/CCMN.2013.0610104

Velbel (1993) hypothesized that during subaerial weathering, the formation of surface layers composed of gibbsite and goethite should have different kinetic consequences and produce different dissolution and replacement textures than surface layers composed of gibbsite and hematite. A surface layer composed of gibbsite and goethite formed by replacement of almandine garnet is predicted to have a volume greater than the volume of the parent almandine garnet replaced (Velbel, 1993). In such a scenario the surface layer has negligible porosity. Negligible porosity requires that transport of soluble species to or from the almandine's surface is restricted to grain-boundary diffusion between product-mineral crystals or volume diffusion through the product-mineral crystal structures. Such a layer thereby inhibits continued garnet dissolution. Reaction kinetics in which the rate-determining process is diffusion of mobile reactant or product species through the medium surrounding the primary mineral are referred to as transport-controlled or transport-limited kinetics, and primary-mineral surfaces affected by transport-limited kinetics are smooth and rounded (Berner, 1978). Solid material through which diffusion is rate limiting is referred to as a protective surface layer (Velbel, 1993; abbreviated herein as PSL). Following previous work using the Pilling-Bedworth criterion, Velbel (1993) defined a surface layer as being protective when the volume of the product(s) formed by replacement of a primary mineral is greater than or equal to the volume of the reactant mineral replaced ($V_p/V_r \geqslant 1$). In contrast, a surface layer composed of gibbsite and hematite formed by replacement of almandine garnet will have a volume significantly less than the volume of the parent almandine garnet replaced (Velbel, 1993) ($V_p/V_r < 1$). In such a scenario the resulting high porosity in, and/or cracks and other voids through, the surface layer allow movement of solvent and solutes to and from the reacting almandine garnet surface. The surface layer has no restricting effect of solvent on solute transport, and does not protect the primary-mineral surface from access by mobile species. Reaction kinetics in which the rate-determining process is reaction at the interface (slower than diffusion of mobile reactant or product species through the medium surrounding the primary mineral) are referred to as surface-controlled or interface-limited kinetics. Primary-mineral surfaces affected by surface-controlled kinetics exhibit crystallographically controlled etch pits (Berner, 1978). A layer of products with these characteristics is referred to here as an unprotective surface layer (USL).

Four tests exist for distinguishing transport-limited from interface-limited kinetics (Berner, 1978) but three apply only to laboratory experiments. Examination of primary-mineral surfaces for smooth or pitted surfaces is the only one of the four tests that can be applied to naturally weathered mineral grains as well as experimental kinetic data (Velbel, 2004). Velbel (1993) tested the hypothesis that different combinations of secondary Fe- and Al-bearing minerals have different consequences for mineral–water reaction kinetics and primary-mineral surface textures. He found broad agreement between the product-reactant volume ratios (V_p/V_r) and textural observations. Specifically, of the major rock-forming silicates, only almandine garnet exhibited both kinetic mechanisms. The product-reactant volume ratios indicated that gibbsite-goethite layers which had been reported by previous workers (*e.g.* Velbel, 1984b, and references therein) formed PSLs over smooth almandine surfaces in saprolites beneath soils. In contrast, products were absent from etched surfaces in soils. Both phenomena had been reported by previous workers; *e.g.* Velbel, 1984b, and references therein. The amount (volume) of product that can be formed upon replacement of a primary mineral by its secondary weathering products depends on the abundances of product-forming elements in the primary mineral. Therefore, the product volume varies with compositional variations in the primary mineral due to elemental substitution in solid-solution. To date Velbel's (1993) hypothesis has not been extended beyond end-member compositions of natural almandine garnets.

The purpose of this study was to test the hypothesis that the kinetic role of almandine garnet's weathering products varies with the composition of the specific almandine experiencing weathering. This hypothesis is tested by calculating the product-reactant volume ratios for natural almandine garnets from Coweeta Hydrologic Laboratory (CHL) in western North Carolina, USA, using the Pilling-Bedworth criterion (Velbel, 1993). In support of this, the formation and nature of surface layers on naturally occurring almandine garnets, including observations of underlying garnet surface textures, are initially characterized. Second, the possible temporal changes in surface layer mineralogy are considered based on the surface textures of naturally weathered almandine garnets in the observational portion of the study. Finally, the possibility of exporting Al derived during almandine garnet surface layer formation, as a function of the different secondary minerals in the surface layer, is presented following work by Velbel *et al.* (2009). Aluminum budgets for the system are determined from the stoichiometric coefficients of Al and Fe in the parent almandine garnet and secondary PSL minerals. Production of PSLs and, subsequently, possible excess Al available for export is a function of the primary almandine garnet's Al and Fe stoichiometric coefficients, molar mass, and specific gravity.

BACKGROUND

Previous work

The rate-determining step of the hydrolysis of silicate minerals during chemical weathering may occur by one of three mechanisms: (1) transport control in which

https://doi.org/10.1346/CCMN.2013.0610104 Published online by Cambridge University Press

either transport of solvents and/or other reactants to, or products from, the dissolving mineral is rate limiting; (2) reaction-, surface-, or interface-control whereby the detachment of ions or molecules from the mineral surface is rate limiting; or (3) a combination of transport- and interface-control (Berner, 1978, 1981; Blum and Lasaga, 1987; Schott and Petit, 1987; Velbel, 2004). In pure transport-controlled dissolution, ions are detached so rapidly from the surface of a crystal that they become concentrated in the solution adjacent to the mineral surface (Berner, 1978, 1981). As a result, dissolution is regulated by transport of these ions *via* advection or diffusion away from the mineral surface. Transport-controlled kinetics includes reactions whose rates are limited by diffusion through a 'leached' layer. The surfaces of minerals dissolving by transport control are smooth, rounded, and featureless (Berner, 1978, 1981; Velbel, 2004). In contrast, during pure interface-controlled dissolution, ion detachment from the mineral surface is so slow that the relatively rapid transport of solutes away from the mineral prevents an increase in ion concentration adjacent to the crystal surface (Berner, 1978, 1981; Schott and Petit, 1987). Under such circumstances, increased advection or diffusion away from the mineral surface has no effect on the dissolution rate (Berner, 1978, 1981). Interface-limited mechanisms result in etch pit formation on mineral surfaces, reflecting the site-selective nature of the interfacial reaction (Wilson, 1975; Berner and Holdren, 1977; 1979; Berner, 1978, 1981; Berner *et al.*, 1980; Berner and Schott, 1982; Brantley *et al.* 1986; Lasaga and Blum, 1986; Blum and Lasaga, 1987). Interface-limited kinetics are now widely accepted for most major rock-forming silicates, including feldspars, pyroxenes, amphiboles, and olivine (Velbel, 1993; Blum and Stillings, 1995; Brantley and Chen, 1995; Brantley, 2005, 2008; Lüttge and Arvidson, 2008).

Velbel (1984a, 1993) described almandine garnet replacement textures and the formation of PSLs developed during chemical weathering. Velbel (1993) determined that protective surface layers can only form if: (1) the immobile elements (*e.g.* Al and Fe) behave conservatively at the scale of the garnet-grain surface; and (2) the volume of product(s) formed during weathering are equal to or greater than the volume of the reacting garnet replaced. Velbel (1984a, 1993) suggested that an almandine with a PSL composed of goethite and gibbsite would experience diffusion-limited dissolution. That is, the rate-determining step during weathering reflects transported-controlled kinetics in the form of diffusion of ions through the PSL, with diffusion being the slowest form of transport (Berner, 1978, 1981). The almandine garnet grains that develop PSLs weather more slowly than the grains which do not (Embrechts and Stoops, 1982; Velbel, 1984a). Almandine garnet surfaces beneath the PSL are smooth and featureless, with rounding of grain corners, reflecting uniform attack on the surface (Berner, 1978, 1981). In contrast, if the surface layer is significantly permeable and unprotective (USL), then diffusion through the open pore network is not sufficiently slow to affect garnet dissolution. Under such circumstances, interface-controlled kinetics is favored with the rate-determining step being processes occurring at the mineral–solution interface, and etch pits form (Berner, 1978, 1981).

Velbel's (1984a, 1993) work on almandine garnet weathering reflects observations for the regolith of the Appalachian Southern Blue Ridge Physiographic Province, USA. In addition to goethite and gibbsite weathering products identified by Velbel (1984a, 1993), hematite has also been observed (Graham *et al.*, 1989a, 1989b, 1990a, 1990b). To date, hematite, goethite, and gibbsite are the only weathering products for almandine garnet reported for the Southern Blue Ridge (Graham *et al.*, 1989a, 1989b, 1990a, 1990b; Velbel 1984a, 1984b, 1993). Despite the release of Si and Al during almandine dissolution, no studies to date have identified kaolinite as a weathering product.

The formation of USLs on hornblende in the Southern Appalachian Blue Ridge Mountains of northeastern Georgia, USA, was investigated by Velbel *et al.* (2009). From hornblende-product molar volume calculations, these authors found that Al must be imported to the hornblende-surface layer system during early-stage weathering. Although Al is typically considered negligibly mobile during weathering, some previous work identified instances of substantial Al mobilization (*e.g.* Gardner, 1992). Velbel *et al.* (2009) suggested that the source of the imported Al in the weathering products of hornblende they studied is from garnet weathering known to occur in the same rock unit. For the textbook end-member almandine garnet composition, Velbel (1993) showed that a PSL may form while up to 15% of the Al and Fe produced during almandine garnet dissolution may be exported from the almandine garnet-PSL microenvironment.

Study area

The study area is the U.S. Forest Service Coweeta Hydrologic Laboratory (CHL) located in the southeastern Blue Ridge Physiographic Province of western North Carolina (Figure 1). The Coweeta Basin is underlain by amphibolite-facies metamorphosed sediments of the Coweeta Group (mid-Ordovician; Miller *et al.*, 2000) and the Otto Formation (Upper Precambrian; Hatcher 1980, 1988). The Coweeta Group is subdivided into three lithostratigraphic units. The basal Persimmon Creek Gneiss is predominantly a massive quartz diorite orthogneiss with interlayers of metasandstone, quartz-feldspar gneiss, and pelitic schist (Hatcher, 1980). The overlying Coleman River Formation is characterized by metasandstone and quartz-feldspar gneiss with lesser pelitic schist and calc-silicate quartzite. The Coleman River Formation is overlain by the Ridgepole Mountain

https://doi.org/10.1346/CCMN.2013.0610104 Published online by Cambridge University Press

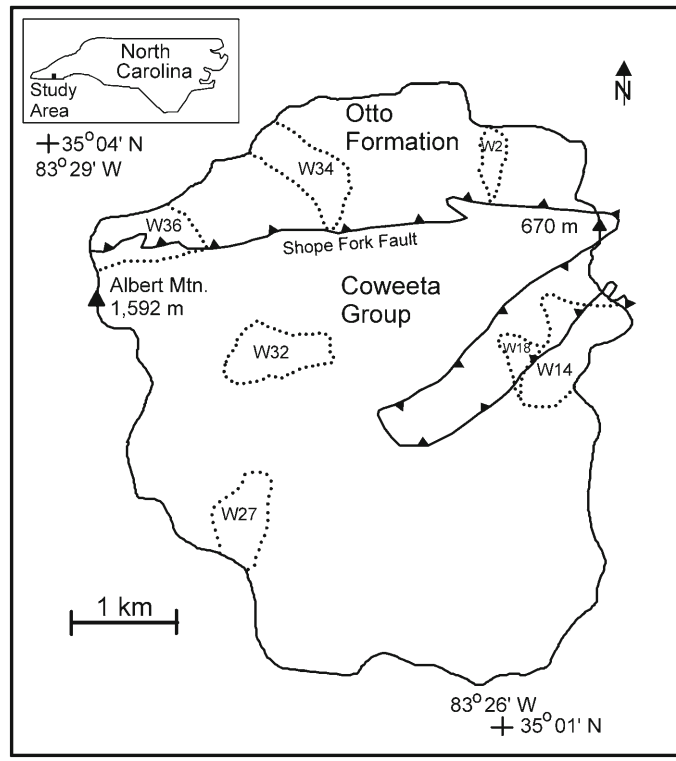

Figure 1. Map of Coweeta Hydrologic Laboratory showing the locations of control watersheds.

Formation; a mineralogically more mature coarse biotite-garnet schist, pelitic schist, metaorthoquartzite, garnetiferous metasandstone, and muscovite-chlorite quartzite (Hatcher, 1980). In contrast to the maturity of the Coweeta Group protolith sediments (*e.g.* arkoses and quartz arenites), the Otto Formation is derived from sedimentary protoliths of low compositional maturity (*e.g.* greywackes) and is feldspar- and biotite-rich (Hatcher, 1980, 1988).

The average weathering profile (saprolite and soil) at Coweeta is ~6 m thick (Berry, 1976; Yeakley *et al.*, 1998). The saprolite at Coweeta is not an ancient, relict, deep weathering profile, as shown by its great thickness (up to 18 m; Berry, 1976; Ciampone, 1995) despite residing on very steep slopes (average slope of ~45%/23°; Velbel, 1985). On such steep slopes, ancient weathering profiles would probably have succumbed to mass wasting and not have survived to the present. Coweeta soils are mostly Ultisols and Inceptisols (Velbel, 1988). Coweeta soils are typically limited in thickness to the uppermost 30 cm of the profile and differ from the underlying saprolite in that they are friable and the residual parent rock structure and fabric have been destroyed by soil forming processes, including transformation or neoformation of soil minerals, mass-wasting, slope creep, root throw, and bioturbation (Velbel, 1985). Soil textures range from fine/coarse loamy, micaceous to fine/coarse loamy, mixed (Browning and Thomas, 1985) and most Coweeta soils are well to extremely well drained. Umbric Dystrochrepts occur at high elevations on steep, rocky north- and south-facing slopes, Typic Dystrochrepts occur on south-facing slopes underlain by the Otto Formation, and Typic Haplumbrepts (Inceptisols) occur on colluvium in hollows and coves. Ultisols have formed in residuum of weathered schists and gneisses and include Typic Hapludults and Humic Hapludults. Typic Hapludults are the most prevalent soil type at Coweeta and are found on sloping ridges and side slopes. Humic Hapludults are found on cooler, steep, north-facing slopes (Swank and Crossley, 1988).

METHODS

Application of the Pilling-Bedworth Rule

The Pilling-Bedworth method was established by metallurgists to explain and predict oxidation products on metals (*e.g.* Kubaschewski and Hopkins, 1962; Hauffe, 1965). Velbel (1993) and Velbel *et al.* (2009) adapted the criterion for application to the chemical weathering of silicate minerals and their possible secondary products, including garnets. The Pilling-Bedworth rule may be important for reaction products in which diffusion of matter is from the outer surface of the product toward the metal–product interface (Kubaschewski and Hopkins, 1962; Fromhold, 1976).

https://doi.org/10.1346/CCMN.2013.0610104 Published online by Cambridge University Press

This geometry is analogous to observed centripetal garnet replacement textures characterized by Velbel (1984a, 1993).

The Pilling-Bedworth criterion applied to the weathering of rock-forming minerals involves calculation of the ratio of the volume of the secondary weathering products (V_p) replacing a primary weathering mineral to the volume of primary mineral replaced (V_r). When $V_p/V_r \geqslant 1$, the surface layer of secondary minerals will occupy at least the same volume as the portion of the reactant mineral replaced. Such a surface layer is pore free and thus a PSL (Kubaschewski and Hopkins, 1962; Hauffe, 1965; Velbel, 1993). Diffusion through a PSL (by grain-boundary diffusion between product-mineral crystals or volume diffusion through the product-mineral crystal structures) is rate determining for the chemical weathering of the reactant mineral. With a PSL the kinetics of the weathering primary mineral are transport- (diffusion)-limited, the mineral grains exhibit sharp, smooth contact with the PSL, and primary grain edges and corners become rounded (Velbel, 1984a, 1993). When $V_p/V_r < 1$, the surface layer of secondary minerals is of insufficient volume to be continuous and uninterrupted, and is, therefore, an USL. An USL yields a primary mineral surface that is vulnerable to direct attack by reacting fluids. Also, with an USL the kinetics of the weathering primary mineral are interface limited, and the mineral grains exhibit etched surfaces (Velbel, 1984a, 1993).

Following the Pilling-Bedworth criterion, as presented by Velbel (1993), the total number of moles of a given element (e) in any arbitrary volume of reactant or product mineral is given by

$$m_{e,i} = \frac{n_{e,i} V_i}{V_i^o} \quad (1)$$

where,

$m_{e,i}$ = total number of moles of element e in mineral i

$n_{e,i}$ = stoichiometric coefficient of element e in mineral i

V_i = volume of mineral i

V_i^o = molar volume of mineral i

Writing equations for i = reactant mineral, r, and for i = product mineral, p, setting $m_{e,r} = m_{e,p}$ (that is, conserving element e such that all of element e present in the reactant mineral is incorporated into the product mineral), and combining the equations for reactant and product minerals, and rearranging, yields:

$$V_p/V_r = \frac{n_{e,r} V_p^o}{n_{e,p} V_r^o} \quad (2)$$

where,

V_p/V_r = the volume of product mineral produced per unit volume of reactant mineral if element e is conserved.

By analogy with the Pilling-Bedworth rule, for a primary rock-forming silicate mineral to form a PSL by replacement, conservation of the least mobile elements such as Fe, Al, and Mn must be assumed (Velbel, 1993).

Molar volumes for reactant garnets (V_r^o) were calculated by dividing the molar mass of a mineral by its specific gravity. In the absence of analytically determined primary-mineral chemistries, molar volumes are available from Smyth and Bish (1988). However, using calculated molar volumes determined from site-specific analyzed mineral chemistries yield more meaningful results for the system being investigated. Molar volumes for secondary products (V_p^o) included in this study (Table 1) are from Smyth and Bish (1988), reported by Velbel (1993, table 1). Secondary products investigated in this study are hematite, goethite, gibbsite, kaolinite, and pyrolusite. These minerals are ubiquitous in the CHL regolith (*e.g.* Velbel, 1984a, 1984b; Price, 2003; Price *et al.*, 2005), and some of these have been reported to be associated with garnet weathering in the southern Appalachian Blue Ridge Physiographic Province (*e.g.* Graham *et al.*, 1989a, 1989b, 1990a, 1990b; Velbel, 1984a, 1984b, 1993) and elsewhere (*e.g.* Embrechts and Stoops, 1982; Parisot *et al.*, 1983; Robertson and Butt, 1997).

Published data for natural almandine garnets

Chemical data from Deer *et al.* (1997) were used to establish a conceptual framework for surface layer formation on natural almandine garnets. These data are ideally suited as Deer *et al.* (1997) not only provide analyses spanning a wide range of natural almandine

Table 1. Stoichiometric coefficients and molar volumes for secondary weathering products characteristic of well leached oxidizing conditions.

Mineral	Formula	Element conserved (e)	n_e	V^o	V^o/n_e
Hematite	Fe_2O_3	Fe	2	30.388	15.194
Goethite	FeOOH	Fe	1	20.693	20.693
Gibbsite	$Al(OH)_3$	Al	1	32.222	32.222
Kaolinite	$Al_2Si_2(OH)_5O_4$	Al	2	99.236	49.618
Pyrolusite	MnO_2	Mn	1	16.708	16.708

Data from Smyth and Bish (1988) and reported by Velbel (1993; his table 1).

https://doi.org/10.1346/CCMN.2013.0610104 Published online by Cambridge University Press

garnet compositions, but also include the garnets' specific gravities with many of their chemical analyses. A total of 18 garnet analyses and associated specific gravities (Table 2) were used in the present study.

All surface-layer calculations in this study assumed conservation of Fe in hematite or goethite, and conservation of Al in gibbsite and/or kaolinite (Velbel, 1993; Table 1). For a PSL composed solely of goethite and kaolinite when $V_p/V_r = 1$ the following equation applies:

$$V_r = V_p = Fe_{Grt}V^o_{Gt} + 0.5Al_{Kln}V^o_{Kln} \quad (3)$$

where,

Fe_{Grt} = Fe stoichiometric coefficient of the garnet; assume that all Fe conserved in PSL goethite

V^o_{Gt} = molar volume of goethite

Al_{Kln} = moles of Al in kaolinite of PSL

V^o_{Kln} = molar volume of kaolinite

All subscripts are the standard mineral symbols of Kretz (1983). Rearranging equation 3 yields

$$Al_{Kln} = (V_r - Fe_{Grt}V^o_{Gt})/0.5V^o_{Kln} \quad (4)$$

In order to determine the quantity of Al needed to form a PSL of goethite, gibbsite, and kaolinite when $V_p/V_r = 1$, a gibbsite term must be added to equation 3 as follows:

$$V_r = V_p = Fe_{Gt}V^o_{Gt} + 0.5Al_{Kln}V^o_{Kln} + Al_{Gbs}V^o_{Gbs} \quad (5)$$

where,

Al_{Gbs} = moles of Al in gibbsite of PSL

Rearranging equation 5 yields

$$Al_{Kln} = (V_r - Fe_{Gt}V^o_{Gt} - Al_{Gbs}V^o_{Gbs})/0.5V^o_{Kln} \quad (6)$$

The excess Al available for export is the difference between the number of moles of Al needed to produce a PSL of goethite, gibbsite, and kaolinite when $V_p/V_r = 1$, and the Al stoichiometric coefficient of the parent garnet.

Almandine garnets from Coweeta Hydrologic Laboratory

Three different almandine garnet compositions have been collected from CHL (Figure 1) (Velbel, 1984a, 1984b; Price, 2003; Price *et al.*, 2005), all of which form PSLs during weathering (Velbel, 1984a, 1984b; Bryan, 1994; Price, 2003; Price *et al.*, 2005). Evaluation of these grains permits further exploration of the conceptual framework for surface-layer formation, direct observations of garnet-surface textures, and production of excess Al associated with almandine garnet weathering.

Pilling-Bedworth criterion. The specific gravity of CHL almandine garnets could not be measured so the average of those reported by Deer *et al.* (1997) of 4.05 was used. Calculations were also made using a specific gravity from Klein and Hurlbut (1999) of 4.32. However, the exact specific gravity value used does not appreciably influence the results, and has no influence on the conclusions of this study.

Field sampling and petrography. Almandine garnet samples examined were collected and described by Velbel (1984a, 1984b), Bryan (1994), Price (2003), and Price *et al.* (2005). Parent rock was collected from outcrops, and regolith samples were collected from roadcuts and hand-augered cores. Samples were collected from saprolite (>60 cm below surface grade (b.s.g.)),

Table 2. Almandine garnet analyses from Deer *et al*. (1997) utilized in the present study (n = 18).

Sample	Si	Al	Al	Fe^{3+}	Ti	Mg	Fe^{2+}	Mn	Ca	O	Specific gravity	Molar mass	V_r
3	5.974	0.026	3.879	0.1	0.014	0.917	4.86	0.116	0.07	24	4.235	966	228
11	5.879	0.121	3.872	0.057	0.062	0.951	4.506	0.247	0.277	24	4.09	962	235
12	6.052	0	3.891	0.083	0.081	0.621	4.29	0.295	0.507	24	4.1	959	234
15	5.789	0.211	3.628	0.227	0.143	0.277	4.414	0.399	0.882	24	4.03	980	243
20	5.984	0.016	3.944	0.082	0.002	0.299	4.1	0.297	1.211	24	4.13	965	234
23	5.984	0.016	3.914	0.061	0.012	1.827	3.929	0.049	0.153	24	3.967	935	236
24	5.937	0.063	3.994	0.103	0	1.51	3.808	0.208	0.301	24	4.08	939	230
25	5.901	0.099	3.837	0.13	0.012	0.44	3.943	0.169	1.465	24	4.067	963	237
26	6	0	3.795	0.217	0.007	0.573	3.698	0.597	1.03	24	4.1	962	235
28	5.923	0.077	3.783	0.232	0.004	1.827	3.664	0.084	0.376	24	3.99	936	235
30	5.871	0.129	3.955	0.056	0.024	2.1	3.541	0.154	0.143	24	4.04	926	229
32	5.948	0.052	3.771	0.19	0.044	0.731	3.4	0.078	1.729	24	3.99	948	238
36	5.942	0.058	3.782	0.208	0.011	0.992	3.172	0.044	1.76	24	3.97	941	237
38	5.843	0.157	3.766	0.206	0.015	0.216	3.16	1.571	1.086	24	4.06	978	241
42	5.937	0.063	3.933	0.036	0	1.065	2.751	0.563	1.6	24	3.99	935	234
43	6.017	0	3.866	0.12	0.018	1.782	2.664	0.085	1.361	24	3.93	916	233
44	5.911	0.089	3.686	0.274	0.03	0.513	2.658	2.331	0.485	24	4.14	977	236
48	5.992	0.008	3.614	0.32	0.017	0.539	1.942	1.487	2.048	24	3.971	954	240

https://doi.org/10.1346/CCMN.2013.0610104 Published online by Cambridge University Press

middle soil horizons (17−60 cm b.s.g.), and upper soil horizons (0−10 cm b.s.g.). Samples were thin sectioned and examined with polarized-light microscopy with weathering textures being photographed with a 35 mm film camera mounted on a petrographic microscope.

Weathered almandine garnets were hand-picked from the >1 mm fraction of the saprolite and soil samples. Samples were washed with deionized water through a 1 mm sieve and the >1 mm fraction dried at 60ºC for 24 h. Almandine garnet grains from the >1 mm regolith fraction and from rock outcrops were hand picked under a binocular microscope.

X-ray diffractometry (XRD). Separation into the <2 mm size fraction was performed by gravity settling, with the <2 mm size fraction being separated with a pipette, and the aliquots being filtered onto a 0.45 μm Millipore™ filter following rapid-suction mounting techniques (production of oriented mounts; also termed the Millipore™ Filter Transfer Method of Drever (1973); this method was described thoroughly by Moore and Reynolds (1997)). Almandine garnet samples and clay minerals in the <2 μm size fraction were initially analyzed by XRD at Michigan State University utilizing a Philips APD (Automated Powder Diffraction) 3720 X-ray diffractometer equipped with an APD 3521 goniometer, a Philips goniometer with CuKα radiation (35 kV, 20 mA), a 1º divergence slit, a 0.2 mm receiving slit, a 1º anti-scatter slit, and a graphite monochromator on the diffracted beam. Almandine garnet samples were step-scanned for various intervals at 0.05º2θ steps using a counting time of 2 s per step.

Additional scans were completed at Franklin and Marshall College, Lancaster, Pennsylvania, using a fully computer-controlled PANalytical X'Pert Pro XRD. Radiation was CuKα (45 kV, 40 mA), with an automated preprogrammed divergence slit that allowed for a constant sample irradiation length of 10 mm, and a 2º anti-scatter slit. Six detectors operated throughout the scan and the sample was rotated continuously during measurement.

Electron microscopy. Hand-picked almandine garnet grains from one or two intermediate points in each profile were mounted to scanning electron microscopy (SEM) stubs with press-on adhesive tabs designed for SEM work. Whole and fractured (by gentle crushing) garnet grains were prepared in the same manner. Grains prepared in this manner were examined by scanning electron microscopy (SEM) in secondary electron imaging (SEI) mode. Polished thin sections of Coweeta bedrock and regolith were imaged using SEM in backscattered-electron imaging (BEI) mode, and energy-dispersive X-ray spectroscopy (EDS). The SEM stubs were gold-coated, and thin sections were either carbon- or gold-coated. Gold-coating of thin sections was often necessary because carbon-coating did not always provide adequate conductivity to prevent sample charging. Imaging and analyses were performed at Michigan State University's Center for Advanced Microscopy (CAM) using a JEOL JSM-35CF SEM. More than 200 micrographs were taken of garnet weathering textures, with the most informative images included herein. Additional photomicrographs may be found in Bryan (1994).

Electron microprobe phase analyses (EMPA). Electron microprobe analyses of Otto Formation, Coleman River Formation, and Ridgepole Mountain Formation garnets in thin section were completed at the University of Michigan's Electron Microbeam Analysis Laboratory (EMAL), using a wavelength dispersive Cameca SX 100 electron microprobe analyzer. The accelerating voltage and beam current were 15 keV and 10 nA, respectively, and a beam diameter of 2 μm was used. Calibration standards for Si, Al, Mg, Fe, Mn, Ti, and Ca were tanzanite (natural), andalusite (natural), enstatite (synthetic), ferrosilite (synthetic), rhodonite (natural Broken Hill), geikielite (natural), and tanzanite (natural), respectively. All garnet formulae reported in this study were reported on an anion basis of O_{24}.

RESULTS

Application of Pilling-Bedworth rule to naturally occurring almandine garnet compositions

None of the 18 almandine garnet samples reported by Deer *et al.* (1997) would produce a PSL of hematite and gibbsite (Table 3). Hematite has a relatively low molar volume per mole of Fe, with V^o/n_e = 30.388/2 = 15.194 (Table 1). Because goethite has V^o/n_e = 20.693, having goethite as the Fe host is more likely to yield a PSL than one in which hematite is the Fe host. Similarly, kaolinite has a greater V^o/n_e value (49.618) than does gibbsite (32.222) (Table 1). Thus, a surface layer in which kaolinite is the Al host is more likely to be protective than one in which gibbsite is the Al host. The importance of the presence of kaolinite in a surface layer is reflected in the fact that 89% of the almandine garnets (Table 3) could form a PSL composed of hematite and kaolinite, despite hematite being the Fe host. To weather to a PSL of hematite and kaolinite, almandine garnet would have to possess minimum Fe and Al stoichiometric coefficients of ~2.8 a.p.f.u. and ~3.78 a.p.f.u., respectively (anion basis of O_{24}) (Figure 2a). Most of the almandine garnets investigated satisfied this criterion (Table 2). In contrast, only one of the 18 almandine garnet samples (6%) reported by Deer *et al.* (1997) (sample 3) had an appropriate chemistry to produce a PSL of solely goethite and gibbsite (Table 3; Figure 2b). Sample 3 producing a PSL of goethite and gibbsite did so because of the garnet's relatively high Fe stoichiometric coefficient (Table 2). This Fe stoichiometric coefficient is above an approximate minimum of ~4.7 (anion basis of O_{24})

https://doi.org/10.1346/CCMN.2013.0610104 Published online by Cambridge University Press

Table 3. Results of surface-layer calculations for garnet compositions and specific gravities, as reported by Deer *et al*. (1997).

Sample	V_p/V_r								Moles of Al needed for $V_p/V_r = 1$ (PSL of goethite + kaolinite)	Excess Al when $V_p/V_r = 1$ (PSL of goethite + kaolinite)
	Hematite + Gibbsite	Hematite + Kaolinite	Goethite + Gibbsite	Goethite + Kaolinite	Hematite + Gibbsite + Pyrolusite	Hematite + Kaolinite + Pyrolusite	Goethite + Gibbsite + Pyrolusite	Goethite + Kaolinite + Pyrolusite		
3	0.88	1.18	1.00	1.30	0.89	1.19	1.01	1.31	2.53	1.38
11	0.84	1.14	0.95	1.24	0.86	1.15	0.97	1.26	2.87	1.12
12	0.82	1.11	0.92	1.21	0.84	1.13	0.94	1.23	2.92	0.97
15	0.80	1.07	0.90	1.18	0.83	1.10	0.93	1.21	3.00	0.84
20	0.82	1.11	0.92	1.21	0.84	1.13	0.94	1.23	2.99	0.97
23	0.79	1.08	0.89	1.18	0.80	1.09	0.89	1.18	3.11	0.82
24	0.83	1.13	0.92	1.23	0.84	1.15	0.93	1.24	3.03	1.02
25	0.80	1.09	0.89	1.18	0.81	1.10	0.90	1.19	3.10	0.84
26	0.77	1.06	0.87	1.15	0.82	1.10	0.91	1.19	3.12	0.67
28	0.78	1.07	0.87	1.16	0.79	1.07	0.88	1.17	3.13	0.73
30	0.81	1.12	0.90	1.21	0.82	1.13	0.91	1.22	3.15	0.94
32	0.75	1.03	0.83	1.11	0.75	1.03	0.84	1.12	3.32	0.51
36	0.74	1.02	0.82	1.10	0.74	1.02	0.82	1.10	3.39	0.45
38	0.74	1.02	0.81	1.10	0.85	1.13	0.92	1.21	3.47	0.45
42	0.73	1.03	0.80	1.09	0.77	1.07	0.84	1.13	3.58	0.42
43	0.72	1.00	0.78	1.07	0.72	1.01	0.79	1.08	3.56	0.31
44	0.70	0.98	0.77	1.05	0.87	1.15	0.94	1.22	3.55	0.22
48	0.63	0.89	0.68	0.94	0.73	0.99	0.78	1.05	Not applicable	
% Forming PSL	0	89	6	94	0	94	6	100		

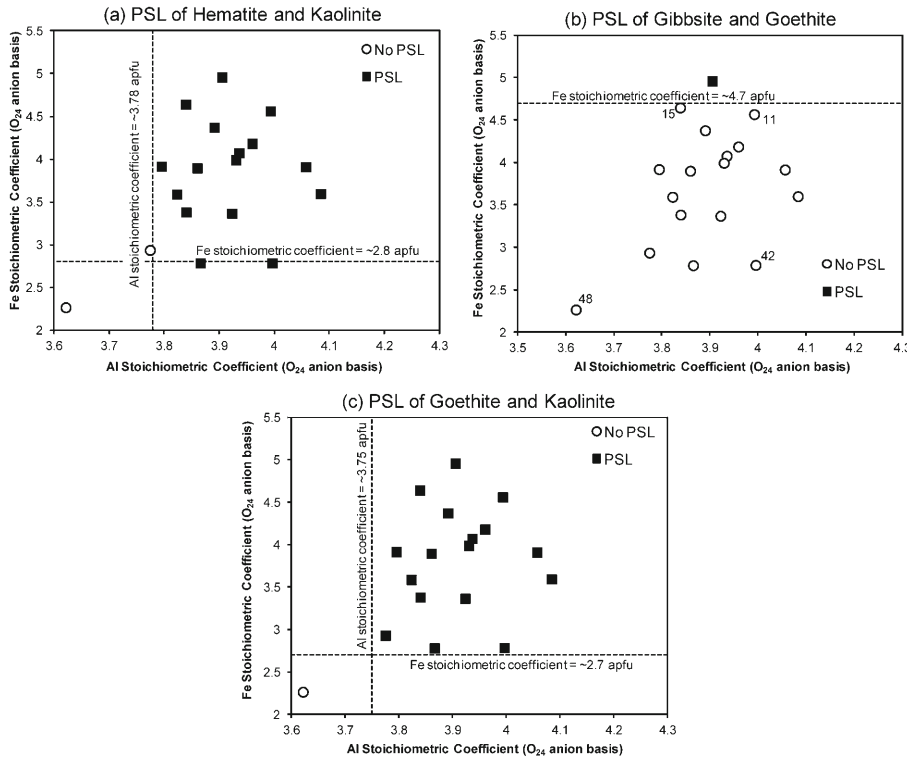

Figure 2. Results of almandine garnet surface-layer calculations for surface layers composed of (a) hematite and kaolinite, (b) goethite and gibbsite, and (c) goethite and kaolinite. 'PSL' indicates that the surface layer is protective, with $V_p/V_r \geqslant 1$. Minimum Fe and Al stoichiometric coefficients needed to produce a PSL are provided.

required for PSL formation (Figure 2b). This is consistent with the V_p/V_r calculations of Velbel (1993) for end-member almandine garnet. Of the remaining samples, all but one (sample 48) would produce a PSL of goethite and kaolinite (Table 3; Figure 2c). This illustrates that formation of PSLs on most naturally occurring almandine garnets requires more complicated combinations of actual primary-mineral compositions and product assemblages than the end-member almandine garnet invoked by Velbel (1993). To form a PSL of goethite and kaolinite an almandine garnet would have to possess a minimum Fe stoichiometric coefficient of ~2.7 a.p.f.u. and a minimum Al stoichiometric coefficient of ~3.75 a.p.f.u. (anion basis of O_{24}) (Figure 2c). These stoichiometric coefficients are only slightly lower than those reported for a PSL composed of hematite and kaolinite (Figure 2a). Adding pyrolusite to the surface layer only increases V_p/V_r to $\geqslant 1$ for one sample (44) when the other product minerals are hematite and kaolinite, and one additional sample (48) when the other product minerals are goethite and kaolinite (Table 3). Therefore, including the volume of pyrolusite formed if Mn behaves conservatively in a surface layer will only modify it from a USL to a PSL for a relatively small number of almandine garnets which host substantial quantities of Mn. However, the only product mineralogy that allows for formation of a PSL on all of the almandine garnets (Table 3) is goethite, kaolinite, and pyrolusite. The influence of the Mn stoichiometric coefficient on formation of PSL is probably far more significant for spessartine garnets which are not evaluated in this study.

All but two of the V_p/V_r values for a surface layer of hematite and kaolinite are >1, and all but one of V_p/V_r values for a surface layer of goethite and kaolinite are >1 (Table 3; Figure 2). V_p/V_r values >1 imply that typically not all of the Fe and/or Al released during garnet weathering is required to be incorporated in the PSL. To address the production of excess Al during almandine garnet weathering (Velbel *et al.*, 2009) and PSL formation, focus was placed on surface layers in which all of the Fe was conserved in the PSL, and the Fe-host was goethite, as this combination had the largest V_p/V_r values (Table 3). Sample 48 had $V_p/V_r < 1$ for a surface layer that included either gibbsite or kaolinite as the Al-host (Table 3) and, thus, has not been included in the evaluation that follows. Using equation 4 above, the minimum number of moles of Al needed to produce a PSL of goethite and kaolinite has been calculated (second to the last column on the right of Table 3). The difference between this value and the Al stoichiometric coefficient of the parent almandine garnet yields the number of moles of Al available for export away from the almandine garnet while the PSL is still preserved (far right column of Table 3). In all 17 samples investigated, the maximum number of moles

https://doi.org/10.1346/CCMN.2013.0610104 Published online by Cambridge University Press

of Al in excess of that required for PSL formation with $V_p/V_r = 1$ was substantial, ranging from 0.22 to 1.38.

The moles of Al released by almandine garnet weathering in excess of that needed to form a PSL using equation 4 was based on a PSL consisting of goethite and kaolinite (Table 3). However, XRD analyses of almandine garnet PSLs reported by Velbel (1984a, 1993) from western North Carolina indicated that gibbsite was ubiquitous in the PSL. Equation 6 was used to explore the relative proportions of gibbsite and kaolinite in a PSL at $V_p/V_r = 1$ in which all of the Fe was conserved in goethite. This relationship was investigated using four Deer *et al.* (1997) samples which represented the following parent garnet scenarios: (1) high Al and high Fe stoichiometric coefficients; (2) low Al and high Fe stoichiometric coefficients; (3) low Fe and high Al stoichiometric coefficients; and (4) low Al and low Fe stoichiometric coefficients. The samples used were 11 (high Al and high Fe stoichiometric coefficients), 15 (low Al and high Fe stoichiometric coefficients), 42 (low Fe and high Al stoichiometric coefficients), and 48 (low Al and low Fe stoichiometric coefficients) (Figures 2b, 3). The almandine garnet Fe stoichiometric coefficient exerted a strong influence on the formation of PSLs (Figure 3, Tables 3, 4). A relatively high almandine garnet Fe stoichiometric coefficient is capable of counteracting a relatively low Al stoichiometric coefficient by creating a PSL relatively rich in goethite and/or hematite. Specifically, sample 15 had a relatively high V_p/V_r value despite having a relatively low Al stoichiometric coefficient.

Using equation 6, the relative proportions of Al hosted by gibbsite and kaolinite were included in the PSL for samples 11, 42, and 15 (Table 4, Figure 4). Sample 48 was not included because it does not form a PSL even when kaolinite is substituted for gibbsite in the PSL (Table 3). As the proportion of gibbsite in a PSL increases relative to kaolinite, the quantity of excess Al available for export decreases (Table 4, Figure 4). For sample 11 with a PSL at $V_p/V_r = 1$, when ~0.70 moles of Al were consumed by kaolinite, and 3.30 moles of Al were consumed by gibbsite, the quantity of excess Al available for export was approximately zero (Table 4, Figure 4). Almandine garnets with relatively high Fe and low Al stoichiometric coefficients (*e.g.* sample 15) were capable of yielding more excess Al than an almandine garnet with relatively high Al and low Fe stoichiometric coefficients (*e.g.* sample 42) (Table 4, Figures 2 and 4).

	High Al	Low Al
High Fe	**DHZ Sample: 11** V_p/V_r: High PSL: Goethite + kaolinite Excess Al: High	**DHZ Sample: 15** V_p/V_r: High PSL: Goethite + kaolinite Excess Al: High
Low Fe	**DHZ Sample: 42** V_p/V_r: Intermediate PSL: Goethite + kaolinite Excess Al: Low to intermediate	**DHZ Sample: 48** V_p/V_r: Low PSL: None Excess Al: None

Figure 3. Matrix displaying the relationship of V_p/V_r, PSL formation, and excess Al available for export as a function of parent almandine garnet relative to Al and Fe stoichiometric coefficients.

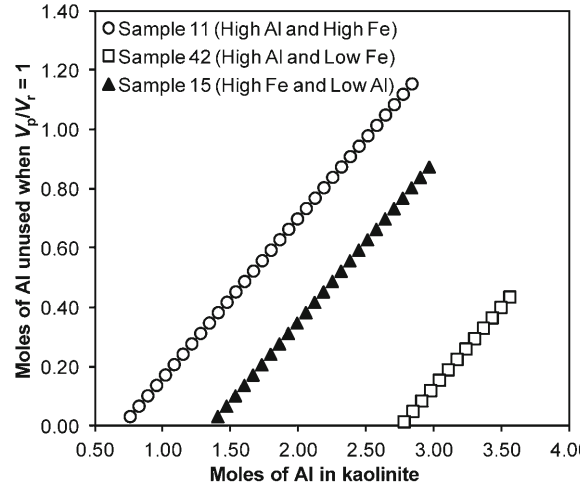

Figure 4. Relationship between Al stoichiometric coefficient of PSL kaolinite and the quantity of excess Al available for export from the almandine garnet-PSL microenvironment. Calculations (Table 4) based on almandine garnet data from Deer *et al.* (1997) (Table 2).

Garnets from Coweeta Hydrologic Laboratory

Mineralogy. Composition data on almandine garnets from the Upper Precambrian Otto Formation and the Mid-Ordovician Coleman River and Ridgepole Mountain Formations are provided in Table 5. X-ray diffractograms of weathered Coweeta almandine garnets displayed peaks indicative of quartz and gibbsite (all samples), hematite (in samples from the warmer, lower elevation Watershed 2), and goethite (in samples from Watersheds 18, 34, and 36) (Bryan, 1994). With the exception of hematite, these results compare favorably with those reported by Velbel (1984a, 1985, 1993). X-ray diffractograms generated as part of this study also yielded peaks for the aforementioned minerals, but also displayed peaks for kaolinite and pyrolusite (Figure 5). Consistent with Bryan (1994), hematite peaks for the Watershed 2 sample (Otto Formation) were taller, sharper, and generally more evident than those for the Watershed 27 sample (Coleman River Formation) (Figures 1 and 5). The same trend was observed for kaolinite.

Pilling-Bedworth Calculations. The methods and Pilling-Bedworth-based concepts outlined above may be applied to almandine garnets found at CHL (Table 5). The results for the CHL garnets are very comparable to

https://doi.org/10.1346/CCMN.2013.0610104 Published online by Cambridge University Press

Table 4. Calculations of excess Al available for export for almandine garnet samples, taken from Deer *et al*. (1997).

– 11 (High Al and high Fe) –			– 42 (High Al and low Fe) –			– 15 (High Fe and low Al) –		
Al_{Gbs}	Al_{Kln}	Excess Al when $V_p/V_r = 1$	Al_{Gbs}	Al_{Kln}	Excess Al when $V_p/V_r = 1$	Al_{Gbs}	Al_{Kln}	Excess Al when $V_p/V_r = 1$
0.00	2.84	1.15	0.00	3.56	0.43	0.00	2.97	0.87
0.10	2.77	1.12	0.10	3.50	0.40	0.10	2.90	0.84
0.20	2.71	1.08	0.20	3.43	0.36	0.20	2.84	0.80
0.30	2.64	1.05	0.30	3.37	0.33	0.30	2.77	0.77
0.40	2.58	1.013	0.40	3.30	0.29	0.40	2.71	0.73
0.50	2.51	0.978	0.50	3.24	0.26	0.50	2.64	0.70
0.60	2.45	0.943	0.60	3.17	0.22	0.60	2.58	0.66
0.70	2.38	0.908	0.70	3.11	0.19	0.70	2.51	0.63
0.80	2.32	0.873	0.80	3.04	0.15	0.80	2.45	0.59
0.90	2.25	0.838	0.90	2.98	0.12	0.90	2.38	0.56
1.00	2.19	0.803	1.00	2.91	0.08	1.00	2.32	0.52
1.10	2.13	0.768	1.10	2.85	0.05	1.10	2.25	0.49
1.20	2.06	0.733	1.20	2.78	0.01	1.20	2.19	0.45
1.30	2.00	0.698	1.30	2.72	−0.02	1.30	2.12	0.42
1.40	1.93	0.663		1.40	2.06	0.38		
1.50	1.87	0.628		1.50	1.99	0.35		
1.60	1.80	0.593		1.60	1.93	0.31		
1.70	1.74	0.558		1.70	1.86	0.28		
1.80	1.67	0.522		1.80	1.80	0.24		
1.90	1.61	0.487		1.90	1.73	0.21		
2.00	1.54	0.452		2.00	1.67	0.17		
2.10	1.48	0.417		2.10	1.60	0.14		
2.20	1.41	0.382		2.20	1.54	0.10		
2.30	1.35	0.347		2.30	1.47	0.07		
2.40	1.28	0.312		2.40	1.41	0.03		
2.50	1.22	0.277		2.50	1.34	0.00		
2.60	1.15	0.242						
2.70	1.09	0.207						
2.80	1.02	0.172						
2.90	0.96	0.137						
3.00	0.89	0.102						
3.10	0.83	0.067						
3.20	0.76	0.032						
3.30	0.70	−0.003						

those of Deer *et al.* (1997) in that the formation of a PSL is very uncommon when the surface layer is composed solely of hematite and gibbsite, or solely of goethite and gibbsite (Table 6). However, a PSL did form in two of three garnets when composed of hematite and kaolinite, and all of the CHL garnets formed a PSL composed of goethite and kaolinite. When V_p/V_r values were above unity, excess Al was available for export. With the exception of the Ridgepole Mountain Formation, adding pyrolusite to a surface layer composed of hematite and kaolinite was insufficient to increase product volume to render an otherwise unprotective layer protective (Table 6). Calculations may also be made when Fe is conserved in goethite and V_p/V_r values are thereby highest, and Al is distributed between gibbsite and kaolinite in a PSL when $V_p/V_r = 1$. The results of these calculations demonstrate that the CHL garnets can possess a PSL of goethite, gibbsite, and kaolinite, and still have significant Al available for export (Table 7, Figure 6). For the Otto Formation garnet, no excess Al will be present when approximately equal molar quantities of Al (~2.0) are distributed between gibbsite and kaolinite (Table 7). Garnet of the Coleman River Formation would have more of the Al hosted by gibbsite than kaolinite when excess Al is zero. The Otto Formation and Coleman River Formation have identical Al stoichiometric coefficients, nearly identical molar masses, and the same specific gravity is used for garnets from both bedrock units. The higher excess Al for the Coleman River Formation reflects its higher Fe stoichiometric coefficients relative to that of the Otto Formation (Table 5). This again illustrates the strong influence of Fe stoichiometry on PSL formation and excess Al when all of the Fe is conserved in a weathering product. The Ridgepole Mountain Formation garnet has the lowest stoichiometric coefficients of both Al and Fe, and would require a PSL relatively rich in kaolinite to yield any excess Al (Table 7).

https://doi.org/10.1346/CCMN.2013.0610104 Published online by Cambridge University Press

Table 5. Data on garnets collected from Coweeta Hydrologic Laboratory. Mineral chemistry for the Otto Formation and the Coleman River Formation from Price *et al.* (2005). Specific gravity reflects an average of 18 samples reported by Deer *et al.* (1997).

Rock unit	Age	Si	Al	Fe	Mg	Mn	Ca	O	Specific gravity	Molar mass	V_r
Otto Formation	Upper Precambrian	6	4	3.52	0.72	1.0	0.82	24	4.05	962	238
Coleman River Formation	Mid-Ordovician	6	4	4.26	0.88	0.44	0.60	24	4.05	968	239
Ridgepole Mountain Formation	Mid-Ordovician	6	3.72	2.82	0.74	0.9	1.74	24	4.05	948	234

Table 6. Results of surface-layer calculations for Coweeta Hydrologic Laboratory almandine garnets.

	V_p/V_r							
Rock unit	Hematite + Gibbsite	Hematite + Kaolinite	Goethite + Gibbsite	Goethite + Kaolinite	Hematite + Gibbsite + Pyrolusite	Hematite + Kaolinite + Pyrolusite	Goethite + Gibbsite + Pyrolusite	Goethite + Kaolinite + Pyrolusite
Otto Formation	0.77	1.06	0.85	1.14	0.84	1.13	0.92	1.21
Coleman River Formation	0.81	1.10	0.91	1.20	0.84	1.13	0.94	1.23
Ridgepole Mountain Formation	0.70	0.97	0.76	1.04	0.76	1.04	0.83	1.10

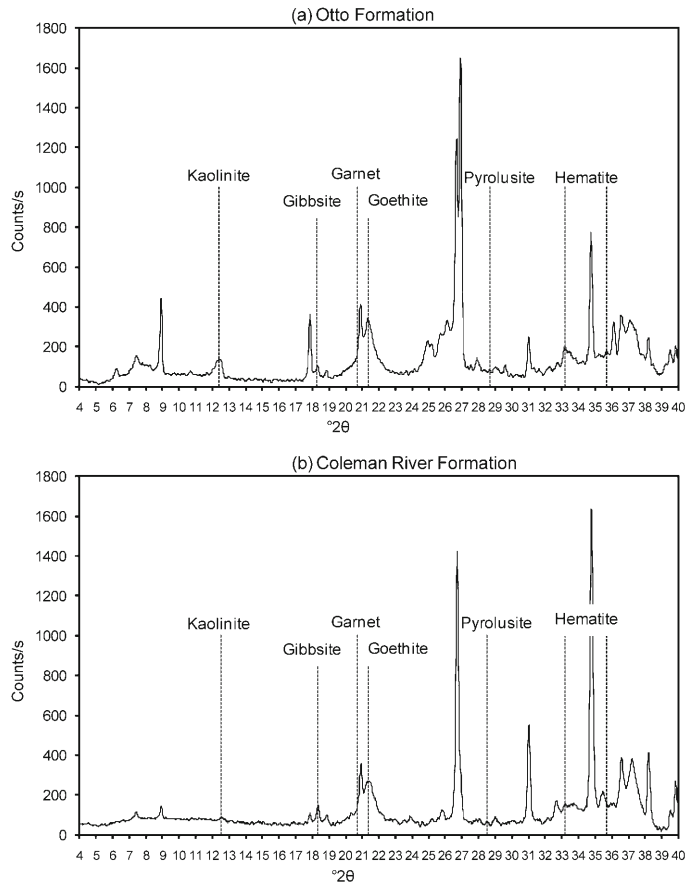

Figure 5. XRD patterns for hand-picked weathered garnet grains from Coweeta regolith. The unlabeled larger peaks include micas (10 Å) and their weathering products and quartz, all of which may be intergrown with garnet grains. Otto Formation samples W2-10, and Coleman River Formation sample W27-7.

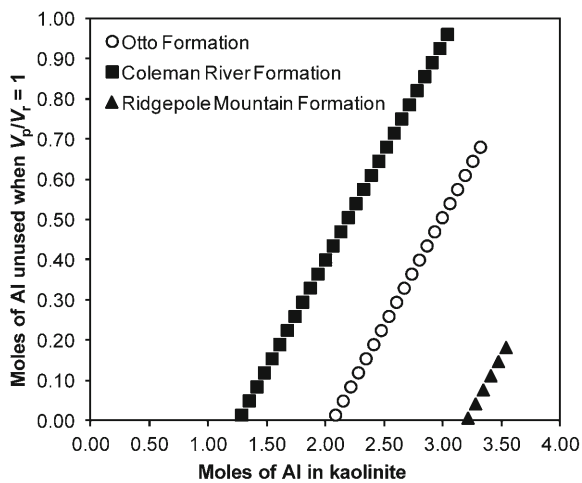

Figure 6. Relationship between Al stoichiometric coefficient of PSL kaolinite and the quantity of excess Al available for export from the almandine garnet-PSL microenvironment for almandine garnets at the Coweeta Hydrologic Laboratory (Table 7).

Energy-dispersive X-ray spectra for CHL almandine garnet from the Otto Formation (Figures 7 and 8) revealed that Si is present in all PSL EDS spectra, probably reflecting the presence of kaolinite identified by XRD (Figure 5). The relative abundance of Si varies depending on the sample and location of the analysis, but variation in brightness of the PSL in a backscattered-electron image indicated that the PSL was not mineralogically homogeneous (Figure 8).

The influence of pyrolusite (Figure 5) on the protectiveness of a surface layer was demonstrated for Coweeta garnets (Table 8). The presence of pyrolusite in the PSL reduces the percentage of Al needing to be hosted by kaolinite by up to 46% (for the Otto Formation; Table 8). Therefore, while pyrolusite in a surface layer may not greatly increase the likelihood of the layer being protective, the presence of pyrolusite does significantly decrease the quantity of kaolinite needed to make a surface layer protective.

Micromorphology of garnets and their surface layers. Garnet grains from CHL exhibited a variety of textures and shapes in thin section. Most garnet grains were

https://doi.org/10.1346/CCMN.2013.0610104 Published online by Cambridge University Press

Table 7. Calculations of excess Al (a.p.f.u.) available for export for almandine garnet samples collected at Coweeta Hydrologic Laboratory.

—— Otto Formation ——			– Coleman River Formation –			Ridgepole Mountain Formation		
Al_{Gbs}	Al_{Kln}	Excess Al when $V_p/V_r = 1$	Al_{Gbs}	Al_{Kln}	Excess Al when $V_p/V_r = 1$	Al_{Gbs}	Al_{Kln}	Excess Al when $V_p/V_r = 1$
0.00	3.32	0.68	0.00	3.04	0.96	0.00	3.54	0.18
0.10	3.26	0.64	0.10	2.98	0.92	0.10	3.47	0.15
0.20	3.19	0.61	0.20	2.91	0.89	0.20	3.41	0.11
0.30	3.13	0.57	0.30	2.85	0.85	0.30	3.34	0.08
0.40	3.06	0.54	0.40	2.78	0.82	0.40	3.28	0.04
0.50	3.00	0.50	0.50	2.72	0.78	0.50	3.21	0.01
0.60	2.93	0.47	0.60	2.65	0.75	0.60	3.15	−0.03
0.70	2.87	0.43	0.70	2.59	0.71			
0.80	2.80	0.40	0.80	2.52	0.68			
0.90	2.74	0.36	0.90	2.46	0.64			
1.00	2.67	0.33	1.00	2.39	0.61			
1.10	2.61	0.29	1.10	2.33	0.57			
1.20	2.54	0.26	1.20	2.26	0.54			
1.30	2.48	0.22	1.30	2.20	0.50			
1.40	2.41	0.19	1.40	2.13	0.47			
1.50	2.35	0.15	1.50	2.07	0.43			
1.60	2.28	0.12	1.60	2.00	0.40			
1.70	2.22	0.08	1.70	1.94	0.36			
1.80	2.15	0.05	1.80	1.87	0.33			
1.90	2.09	0.01	1.90	1.81	0.29			
2.00	2.02	−0.02	2.00	1.74	0.26			
			2.10	1.68	0.22			
			2.20	1.61	0.19			
			2.30	1.55	0.15			
			2.40	1.48	0.12			
			2.50	1.42	0.08			
			2.60	1.35	0.05			
			2.70	1.29	0.01			
			2.80	1.22	−0.02			

embayed or euhedral, and highly fractured. Large crystals were inclusion rich (poikiloblastic), containing (in order of decreasing abundance) quartz, magnetite, biotite, muscovite, chlorite, and epidote. Many internal fractures originated near inclusions (Embrechts and Stoops, 1982) and radial fractures (Wendt *et al.*, 1993) occurred near some quartz inclusions. Other fractures occurred across embayments in rocks with strong preferred orientation and compositional banding. The fractures were perpendicular to foliation and are parallel to each other.

Ferruginous surface layers formed on most weathered almandine garnet grains. Continuous surface layers were more prevalent on euhedral, inclusion-poor grains and on grains that were extremely weathered. Discontinuous surface layers were more prevalent on embayed, inclusion-rich grains and on grains which border iron-rich phyllosilicates (chlorite or biotite). In these instances, weathering products were "co-mingled" with those from the surrounding chlorite or biotite minerals. Orange, red, and yellow-brown ferruginous deposits formed surface layers and boxworks along internal

Table 8. Calculations illustrating the influence of pyrolusite on Al distribution in PSLs ($V_p/V_r = 1$) for almandine garnet samples collected at Coweeta Hydrologic Laboratory.

Rock Unit	% Al in kaolinite for PSL of goethite + gibbsite + kaolinite	% Al in kaolinite for PSL of goethite + gibbsite + kaolinite + pyrolusite	% Difference
Otto Formation	52	28	46
Coleman River Formation	32	21	34
Ridgepole Mountain Formation	86	63	27

https://doi.org/10.1346/CCMN.2013.0610104 Published online by Cambridge University Press

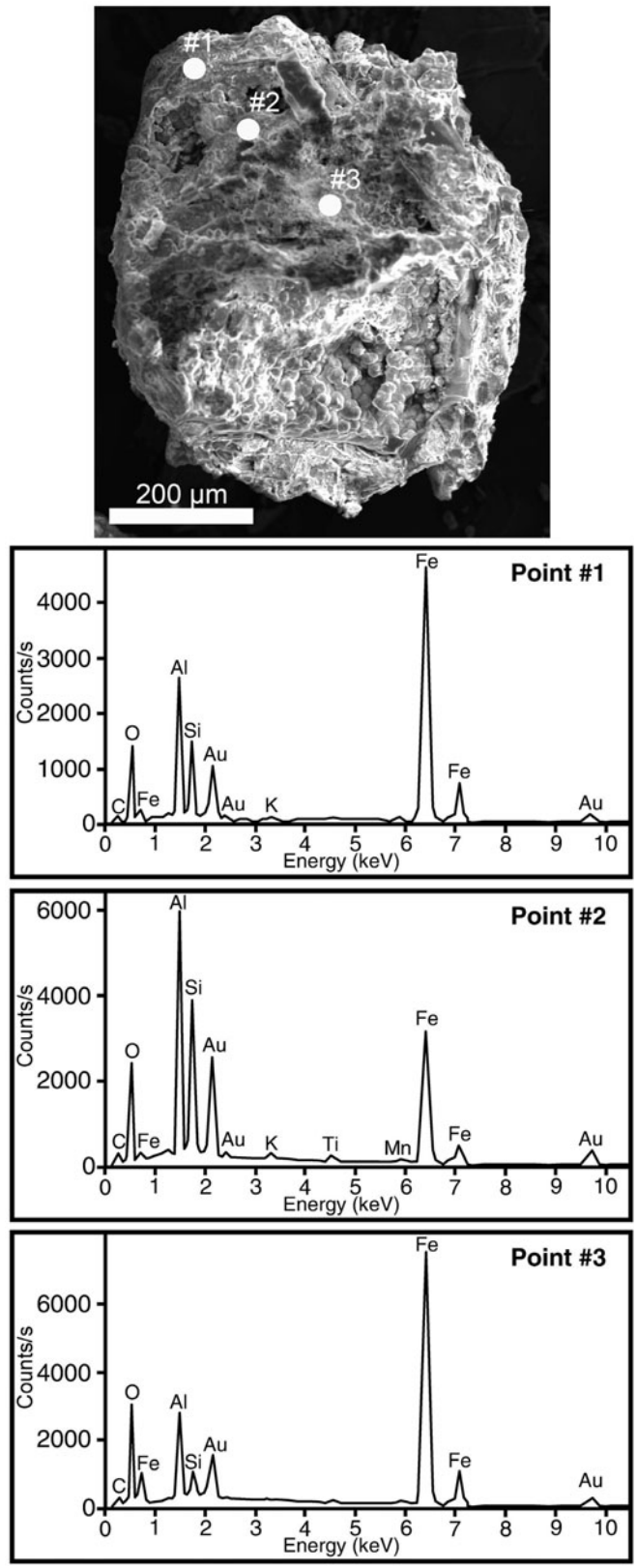

Figure 7. SEM-SEI image and EDS spectra of an Otto Formation garnet with surface layer hand picked from the regolith. Note the presence of Si in all spectra. Sample W34-6.

https://doi.org/10.1346/CCMN.2013.0610104 Published online by Cambridge University Press

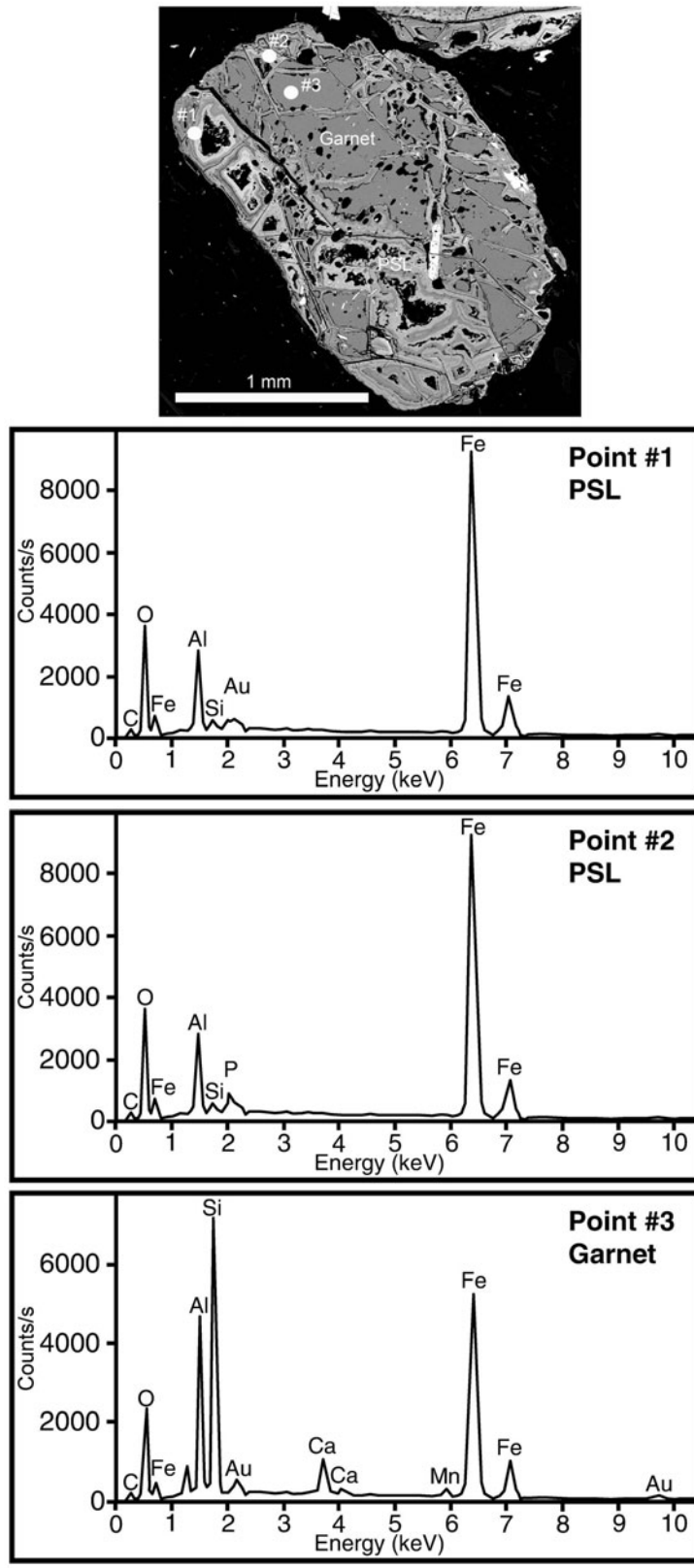

Figure 8. SEM-BEI image and EDS spectra of an Otto Formation garnet with surface layer. Points #1 and #2 are from the PSL and Point #3 is the unweathered garnet. Note the presence of Si in both PSL spectra. Sample W2-5.

https://doi.org/10.1346/CCMN.2013.0610104 Published online by Cambridge University Press

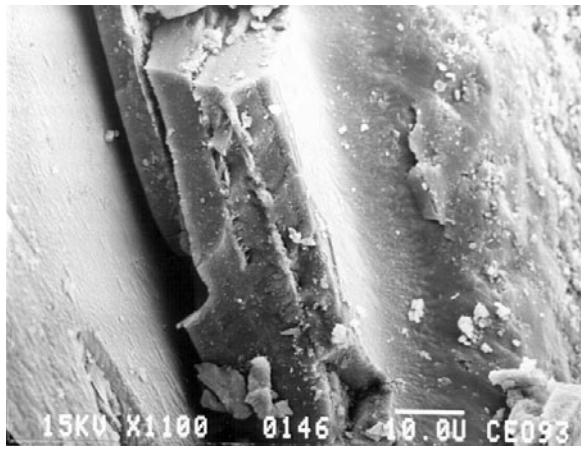

Figure 9. SEM-SEI image of 'onion skin-like' appearance of PSL on almandine garnet. Scale bar is 10 μm.

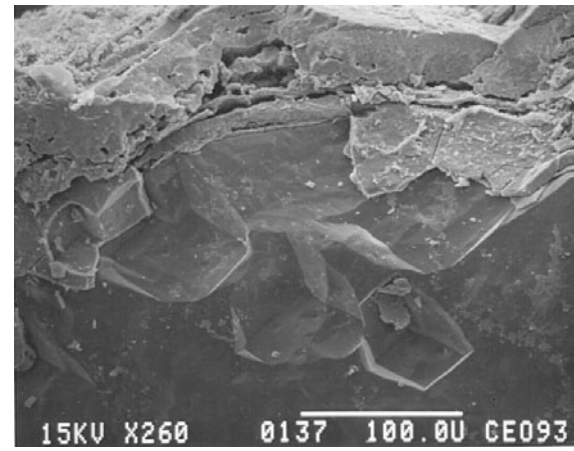

Figure 11. SEM-SEI image of dodecahedral etch pits on almandine garnet preserved in negative relief directly beneath a PSL. Scale bar is 100 μm.

fractures. In some thin sections, ferruginous deposits originating from a garnet occurred in rock fractures and stain surrounding unweathered minerals, suggesting that some garnet weathering products were being transported away from garnet grain boundaries.

Weathered almandine garnets from Coweeta exhibited both PSLs and USLs depending on sample locality and depth. Protective surface layers were the most common, exhibited minimal porosity, and were thickest in the saprolite and decreased in thickness higher in the soil profile. Protective surface layers were continuous over the entire grain surface and had no microporosity perpendicular to grain surfaces, no microporosity parallel to grain surfaces in outcrop samples, and minor (0.8–>5.0 mm in width) microporosity parallel to grain surfaces in profile samples. A PSL may become discontinuous and/or separated from the garnet's surface, probably due to dissolution and abrasion and have an 'onion skin-like' appearance in which successive layers are deposited in contact with previous layers (Figure 9).

Despite being protective as determined from V_p/V_r ratios, some occurrences of surface layers were found covering euhedral (dodecahedral) etch pits on subjacent garnets. Some etch pits were directly observable (Figures 10 and 11), others were preserved as casts on the undersides of the product layers (Figure 12). Unprotective surface layers only occurred in the warmer, dryer Watershed 2 (Figure 1), were more porous, and may have contained relatively high concentrations of hematite (Figure 5). An USL was continuous over the entire grain surface and had microporosity perpendicular to grain surfaces (pores of 8.0–10.0 mm in diameter) and little or no microporosity parallel to the grain surface. Unprotective surface layers were thickest in the upper

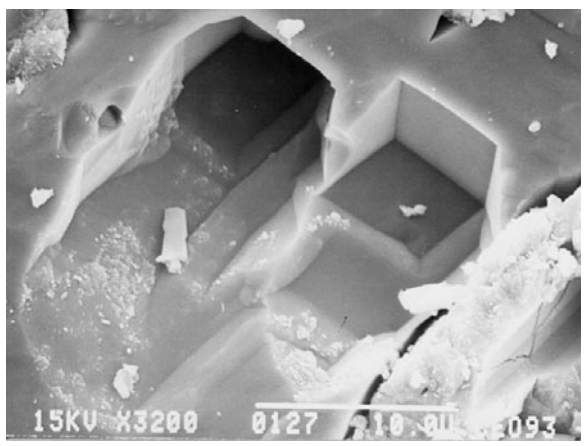

Figure 10. SEM-SEI image of dodecahedral etch pits on almandine garnet. Scale bar is 10 μm.

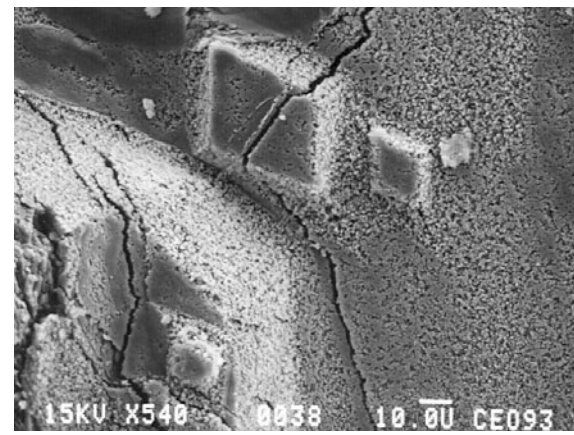

Figure 12. SEM-SEI image of casts of euhedral etch pits preserved in positive relief on the base of PSL separated from an almandine garnet–PSL interface by sample preparation. Scale bar is 10 μm.

https://doi.org/10.1346/CCMN.2013.0610104 Published online by Cambridge University Press

horizons and decreased in thickness lower in the soil profile.

DISCUSSION

Application of Pilling-Bedworth rule to natural almandine garnet compositions

The results above indicate that very few natural almandine garnets have compositions sufficiently close to end-member almandine to allow the formation of PSL consisting of only goethite and gibbsite as suggested by Velbel (1984a, 1993). Based on the findings of the present study, in nearly all naturally occurring almandine garnets, some kaolinite likely must be present in a surface layer to make it protective. The addition of pyrolusite to the surface layer is capable of dramatically lowering the fraction of kaolinite required to make a PSL (Table 8). However, the addition of pyrolusite does not appear to be capable of completely eliminating the need for kaolinite within a PSL.

Micromorphology of CHL garnets and their surface layers

Ferruginous weathering products on naturally weathered saprolite almandine garnets exhibiting rounded and featureless surfaces and having calculated $V_p/V_r \geqslant 1$ have been interpreted as being a PSL. In contrast, etch pits on naturally weathered soil almandines have been interpreted to indicate interface-limited reaction processes (Velbel, 1984a, 1993; Velbel *et al.*, 2007). Garnet etch pits (*e.g.* Figure 10) formed in the absence of PSLs occur in a variety of soil types, apparently where pedogenic complexing agents mobilize Al and/or Fe, and thereby prevent the formation of PSLs (Velbel, 1984a; Ghabru *et al.*, 1989; Velbel *et al.*, 2007). The occurrence of etch pits (Figure 11) and etch-pit casts (Figure 12) in association with surface layers reported here for the first time requires reexamination of the relationship between specific secondary minerals and the rate-determining processes associated with those minerals. Two possible explanations for the presence of PSL-associated etch pits and etch-pit casts are offered: (1) almandine garnet weathers first to a USL followed by mineralogical changes yielding a PSL (*e.g.* hematite hydrating to goethite; Schwertmann, 1971; Campbell and Schwertmann, 1984); or (2) almandine weathers to a surface layer in a mixed-kinetic regime. Each of these possible scenarios is explored below.

Conversion of a USL to a PSL. The presence of a PSL covering etch pits (Figures 11, 12) implies that the surface layer was not diffusion limiting at the time of etch-pit formation, but rather almandine garnet weathering was interface limited. These observations, combined with the Pilling-Bedworth calculations permit the hypothesis that secondary hematite formed at the onset of garnet weathering, forming a USL that allowed rapid solute transport. In the cooler, wetter localities found at the higher elevations of CHL, the early-formed hematite subsequently hydrated to form (tertiary) goethite in a PSL. In virtually all CHL sample sites, almandine garnet is weathering to predominantly goethite (*e.g.* Figure 5). Goethite has also been identified as a predominant weathering product of almandine garnet at other sites (Embrechts and Stoops, 1982; Parisot *et al.*, 1983; Velbel, 1984a; Graham *et al.* 1989a; Robertson and Butt, 1997). The molar volume per Fe is greater for goethite than for hematite (Table 1), and the hydration of Fe products caused a volume increase. This volume increase allowed the hydrated products to occupy formerly vacant space, reducing porosity and thereby filling etch pits and forming casts (Figure 12). The increase in product volume as the goethitic surface layer became protective caused by the hydration process would fill or cover pre-existing etch pits and would prevent additional etch pits from forming.

Based on the discussion above, drawing mechanistic inferences from product mineralogy alone (without information on textural relationships, *e.g.* centripetal replacement textures) is hazardous. For instance, hematite is believed to form from almandine garnet in at least some Southern Blue Ridge weathering profiles (Graham *et al.*, 1989a, 1989b, 1990a, 1990b), and has been identified in the Coweeta PSLs (Figure 5). If almandine garnet weathered directly to secondary hematite, Velbel's (1993) calculations and those as part of this study (Table 6) would suggest that the hematite-bearing product is far less likely to yield a PSL, especially in combination with gibbsite as the sole Al-bearing product. In the present study, etch-pit casts occur only with a PSL containing goethite as the dominant ferruginous product. While no direct evidence of a hematite precursor for these specific goethites was observed, such transformations between hydrous and anhydrous iron oxides are common in weathering environments (*e.g.* Schwertmann, 1971; Campbell and Schwertmann, 1984), and hematite has formed during the weathering history of CHL saprolites (*e.g.* Figure 5). Textural evidence such as etch-pit casts preserve remnant reactant garnet surface textures and suggest, in such instances, both the pathway of goethite formation and the change over time in the rate-determining role of the product. Thus, in the absence of information from replacement textures, the present mineralogy alone of a product assemblage with $V_p/V_r < 1$ is not a sufficient criterion for dismissing the protective surface layer hypothesis, or for confirming that the product itself was not rate determining.

Temporal changes in surface layer mineralogy and kinetic regime are not limited to the Fe-bearing phases hematite and goethite. The Pilling-Bedworth calculations indicate that a PSL is unlikely to form in the absence of kaolinite when gibbsite is the sole aluminous phase. Gibbsite has also been identified as a weathering

https://doi.org/10.1346/CCMN.2013.0610104 Published online by Cambridge University Press

product of garnet by previous workers (Velbel, 1984a; Graham *et al.*, 1989a, 1989b, 1990b). However, to transition from interface-controlled to diffusion-controlled kinetics would require the silication of a 0:1 clay (*i.e.* gibbsite). Typically, with progressive weathering, kaolinite will desilicate to gibbsite. Following this premise, kaolinite would probably form at the beginning of garnet weathering, although some desilication could occur afterwards as long as adequate kaolinite remained to maintain the PSL. Excess Si associated with garnet weathering to a PSL (discussed in the next section) would be available for silication of gibbsite. However, conservation of Si in the almandine garnet-surface layer system would probably only occur with a PSL already present, *i.e.* when Si loss was inhibited by diffusion through the PSL. Based on this reasoning, a conversion from a USL to a PSL, and associated change from interface-controlled to transport-controlled kinetics, would be the more likely result of hematite hydrating to goethite with some kaolinite already present in the surface layer.

Mixed-kinetic control. Weathering regimes which form both etch pits and protective surface layers might be intermediate between transport- and interface-limited kinetic regimes (the mixed-kinetics regime of Berner, 1978, 1981). Where a PSL is slightly discontinuous (Figure 9), interface-limited weathering reactions operate and etch pits form (Figure 11).

Unprotective surface layers increase in thickness higher in the weathering profile. This observation indicates that garnets with USLs weather by centripetal replacement. Almandine garnet grains with USLs appear to have no dissolution features (*e.g.* etch pits) on their surfaces, although the etch pits may be covered by the oxides which form a USL. As reported by Velbel (1984a) and Embrechts and Stoops (1982), regardless of type of surface layer that may form by weathering in the saprolite prior to pedogenesis, almandine garnet weathering in soil horizons proceeds with the formation of a USL which is commonly removed completely with continued pedogenesis in soil horizons (Velbel, 1984a; Ghabru *et al.*, 1989; Velbel *et al.*, 2007).

The two aforementioned explanations of the occurrence of etch pits under a PSL offer plausible explanations for the previously unreported and unexpected weathering texture of etch pits covered by a subsequent layer of secondary (or tertiary) products (Figure 11). The almandine garnet grain was removed directly from rock outcrop. The almandine garnet surface layer is discontinuous and may be so because of mechanical separation from the surrounding matrix or because the surface layer is still forming. The surface layer did form well below the rooting zone and is not discontinuous due to biochemical dissolution. Also, because the almandine garnet was removed from outcrop, the etch pits were not covered by products as a result of direct introduction into the rooting zone followed by reburial. The most probable explanations are that the etch pits formed during preliminary dissolution of the almandine garnet surface and were later filled by the products of the replacement process, or formed while the almandine garnet surface was covered by a porous, hematitic surface layer and were later filled by goethite as the hematite hydrated. The morphological consequences of the last part of this proposed sequence of phenomena may be expressed and preserved at the inner margin of a PSL where it is in direct contact with, and forms a cast of, the etched almandine surface (Figure 12).

Elemental imports and exports for the CHL almandine garnet-PSL system

A surface layer composed of goethite, gibbsite, and kaolinite would probably be protective. Furthermore, an excess of Al is feasible and thus available for export. Velbel (1993) determined that up to 15% of the Al and Fe produced during almandine garnet weathering could be exported from the garnet-PSL microenvironment. For the almandine garnet compositions from Deer *et al.* (1997) used in the present study, up to 35% of the Al produced during almandine garnet weathering may be exported. Such a large value is only possible if all of the Fe is conserved and substantial quantities of kaolinite are present in the PSL. However, petrographic observations reveal that occasionally ferruginous material will extend from a garnet grain into fractures and around adjacent minerals. Migration of Fe from a garnet grain indicates that the assumption of conservation of all almandine garnet-derived Fe in the surface layer may not be valid for some grains. If the quantity of Fe available for surface layer is reduced, then the proportion of kaolinite in a PSL would have to increase relative to gibbsite. This relative increase in PSL kaolinite would also reduce the quantity of Al available for export from the almandine garnet-surface layer microenvironment.

Velbel *et al.* (2009) investigated the formation of USL on hornblende sampled from regolith of the southern Appalachian Blue Ridge of northeastern Georgia, USA. Using similar molar volume calculations as this study, these authors determined that Al must be imported into early-stage weathering products of the hornblende. During the early stages for weathering, considerable mobilization of Al occurred while Si was immobile, despite Al typically being considered minimally mobile during weathering. Velbel *et al.* (2009) suggested that Al is mobilized from shallow depths to greater depths in the weathering profile where incipient weathering is occurring. Further, Velbel *et al.* (2009) proposed that the source of the imported Al is from almandine garnet weathering known to occur in their rock unit of study, although no unweathered almandine garnet was observed in their specific sample. Velbel *et al.* (2009) showed how the proposed Al mobility is consistent with the results of Gardner (1992), White *et*

https://doi.org/10.1346/CCMN.2013.0610104 Published online by Cambridge University Press

al. (1998), and Schroeder *et al.* (2000) based on bulk-sample-scale and profile-scale mineralogical data, solid-phase bulk-chemical analyses of saprolitic weathering profiles, and solute-phase chemical data from soil solutions, groundwater, and modern surface water associated with deeply weathered landscapes.

The possibility of import of element(s) into the almandine garnet-PSL system also warrants investigation. For Coweeta almandine garnets, the balanced weathering reactions for a PSL of goethite and kaolinite, thereby reflecting the maximum production of excess Al (Tables 3 and 7), are as follows:

Otto Formation.

$$Ca_{0.82}Mg_{0.72}Mn_{1.0}Fe_{3.52}Al_4Si_6O_{24} + 7.88\ H_2O + 5.12\ H^+ + 1.41\ O_2 \rightarrow 3.52\ FeOOH + 1.66\ Al_2Si_2O_5(OH)_4 + 2.68\ H_4SiO_4 + 1.0\ MnO_2 + 0.82\ Ca^{2+} + 0.72\ Mg^{2+} + 0.68\ Al^{3+} \quad (7)$$

Coleman River Formation.

$$Ca_{0.60}Mg_{0.88}Mn_{0.44}Fe_{4.26}Al_4Si_6O_{24} + 8.17\ H_2O + 5.84\ H^+ + 1.38\ O_2 \rightarrow 4.26\ FeOOH + 1.52\ Al_2Si_2O_5(OH)_4 + 2.96\ H_4SiO_4 + 0.44\ MnO_2 + 0.60\ Ca^{2+} + 0.88\ Mg^{2+} + 0.96\ Al^{3+} \quad (8)$$

Ridgepole Mountain Formation.

$$Ca_{1.74}Mg_{0.74}Mn_{0.90}Fe_{2.82}Al_{3.72}Si_6O_{24} + 7.12\ H_2O + 5.50\ H^+ + 1.05\ O_2 \rightarrow 2.82\ FeOOH + 1.77\ Al_2Si_2O_5(OH)_4 + 2.46\ H_4SiO_4 + 0.90\ MnO_2 + 1.74\ Ca^{2+} + 0.74\ Mg^{2+} + 0.18\ Al^{3+} \quad (9)$$

These balanced reactions for the formation of a goethite and kaolinite PSL demonstrate that no other major elements need be imported into the PSL-garnet system at Coweeta. However, significantly more Si than Al is released, providing the elements needed to form kaolinite. For the Al to be exported rather than consumed as either kaolinite and/or gibbsite precipitate, the pore solutions must be undersaturated with respect to these phases.

Evaluation of the hypothesis and unresolved issues

The hypothesis for this study was that the role of the kinetics of almandine garnet's weathering products varies with the composition of the specific almandine experiencing weathering. The results of the Pilling-Bedworth calculations and microtextural observations of naturally weathered garnet surfaces from all levels in the CHL weathering profile are consistent with this hypothesis.

The findings of this study yield numerous additional unresolved issues regarding the formation of surface layers on garnets during chemical weathering. The temporal changes in surface-layer mineralogy that may result in etch pits occurring beneath PSLs requires additional investigation. This includes the hypothesized conversion of early-formed hematite to goethite, and the potential role of Si in conversions between gibbsite and kaolinite. Such mineralogical changes should be related directly to the surface microtextures of the dissolving garnet and Pilling-Bedworth calculations. The generation and mobility of Al during incipient garnet weathering, and the potential uptake of that Al by the weathering products of other primary minerals, also warrant further investigation. All of the methods and unresolved questions outlined in this study for almandine garnets may also be applied to garnets representing a wider range of compositions (*e.g.* other garnet solid-solution series) and environmental settings.

SUMMARY AND CONCLUSIONS

The mineralogy of surface layers exerts a major influence on the chemical weathering kinetics of almandine garnet; different product minerals occupy different proportions of the replacement volume and thereby influence the solute-transport properties of the product. During chemical weathering, almandine garnet grains can develop either protective or unprotective surface layers depending on the almandine garnet's Al and Fe stoichiometric coefficients, molar mass, specific gravity, mineralogy of secondary products, and environmental conditions. The results of this study are consistent with the hypothesis that the role of the kinetics of almandine garnet's weathering products varies with the composition of the specific almandine garnet experiencing weathering. Most natural almandine garnets lack adequate Fe and Al to form PSLs composed only of goethite and gibbsite. Having kaolinite in a surface layer dramatically increases the probability of a surface layer being protective. At CHL for almandine garnets from the three units studied, in order to form a PSL, kaolinite must be a weathering product. The lack of kaolinite being reported in the literature may be due to inadequacy of XRD. Energy-dispersive X-ray spectra and XRD analyses as part of this study support the presence of kaolinite in Coweeta almandine garnet PSLs. The greatest likelihood that a surface layer will be protective is when it contains goethite, kaolinite, and pyrolusite. With adequate Mn in the parent garnet and if pyrolusite precipitates in the PSL, the V_p/V_r value will increase. However, pyrolusite in a surface layer may not increase greatly the likelihood of the layer being protective; the presence of pyrolusite does significantly decrease the quantity of kaolinite needed to make a surface layer protective.

Based on an almandine garnet anion basis of O_{24}, to form a PSL composed of hematite and kaolinite, an almandine garnet must have a minimum Al stoichiometric coefficient of ~3.78 a.p.f.u. and a minimum Fe stoichiometric coefficient of ~2.8 a.p.f.u. To form a PSL of goethite and kaolinite, an almandine garnet must have a minimum Al stoichiometric coefficient of

https://doi.org/10.1346/CCMN.2013.0610104 Published online by Cambridge University Press

~3.75 a.p.f.u. and a minimum Fe stoichiometric coefficient of ~2.7 a.p.f.u. A relatively large parent garnet Fe stoichiometric coefficient is more important in PSL formation and determination of excess Al than is the parent almandine garnet Al stoichiometric coefficient.

Almandine garnet and ferruginous product(s) in thin section form three distinct textures: (1) grains in which ferruginous product is in contact with the garnet remnant; (2) grains in which ferruginous product is not in contact with the almandine garnet remnant (formation of a peripheral void around remnant); and (3) grains in which ferruginous product has formed a porous pseudomorph after garnet. Almandine garnet grains in environments dominated by biochemical processes and advective flow undergo interface-limited reactions. Almandine garnet grains in environments not dominated by these processes experience supersaturation with respect to iron and aluminum products near the grain surface. When the requirements for nucleation are met, the products reprecipitate to form a PSL.

Etch pits occur on almandine garnet grains beneath some PSLs. This association of etch pits (which indicate interface-limited kinetics) and PSLs (which should inhibit transport of mobile species to and/or from the almandine's surface, result in reaction kinetics limited by transport through the product, and thereby prevent the formation of etch pits) is unexpected based on the original formulation of the hypothesis. The Pilling-Bedworth calculations of this study suggest a modification of the hypothesis. Several combinations of changes of secondary minerals into tertiary minerals could result in the newly reported association between etch pits (formed in the kinetic regime influenced by the secondary minerals) and PSLs (consisting of tertiary minerals modified from the secondary minerals after the etch pits formed). Early-formed (secondary) product minerals formed USLs and allowed interface-limited attack upon, and etching of, the underlying almandine garnet's surface. This was followed by modification of the secondary product minerals to tertiary product minerals with increased volume that rendered the surface layers protective of the underlying surface after the etch pits had formed.

Several secondary-tertiary product-mineral paragenetic sequences are consistent with this time-variant extension of the original hypothesis. Filled etch pits under PSLs may be the result of hematitic surface layers hydrating to goethitic surface layers or the result of dissolution-reprecipiation processes. The initial formation of hematite in an USL, followed by hydration of hematite to form goethite, reduces porosity. Consequently, the product's transport properties are reduced such that the previously USL of product becomes a PSL only after the etch pits had formed. Similarly, the silication of gibbsite to kaolinite after initial formation of an USL in which Al was hosted by gibbsite would increase product volume, reduce porosity, and change the rate-determining process only after the etch pits had formed. Alternatively, almandine garnet dissolution processes which form PSLs and etch pits may be intermediate between transport- and interface-limited kinetic regimes (Berner, 1978; 1981). Discontinuous surface layers permit the formation of etch pits.

With a PSL of goethite, gibbsite, and kaolinite, excess Al may reasonably be assumed to be available for export. A reduction in the quantity of kaolinite in a PSL resulting from the presence of pyrolusite increases the quantity of Al available for export from the garnet-PSL system. For CHL garnets with PSL and excess Al, no other element need be imported into the garnet-PSL system to produce the observed weathering-product mineral assemblages.

ACKNOWLEDGMENTS

The authors thank S. Anderson, R. Schaetzl, D. Schulze, E. Danielewicz, S. Flegler, D. Mokma, C. Basso, W. Swank, and the staff at the Coweeta Hydrologic Laboratory. Appreciation is also expressed to S. Sylvester at Franklin & Marshall College for assistance with XRD. The present study was funded in part by a grant from The Clay Minerals Society to D. Bryan. Thanks, too, to Editor-in-Chief J.W. Stucki and Associate Editor W.D. Huff for editorial handling, as well as two anonymous reviewers whose constructive reviews greatly strengthened this manuscript.

REFERENCES

Berner, R. (1978) Rate control of mineral dissolution under earth surface conditions. *American Journal of Science*, **278**, 1235–1252.

Berner, R. (1981) Kinetics of weathering and diagenesis. Pp. 111–134 in: *Kinetics of geochemical processes* (A. Lasaga and R. Kirkpatrick, editors). Reviews in Mineralogy, **8**, Mineralogical Society of America, Washington, D.C.

Berner, R.A. and Holdren, G.R. (1977) Mechanism of feldspar weathering: Some observational evidence. *Geology*, **5**, 369–372.

Berner, R.A. and Holdren, G.R. (1979) Mechanism of feldspar weathering II: Observations of feldspar from soils. *Geochimica et Cosmochimica Acta*, **43**, 1173–7786.

Berner, R. and Schott, J. (1982) Mechanism of pyroxene and amphibole weathering II. Observations of soil grains. *American Journal of Science*, **282**, 1214–1231.

Berner, R., Sjoberg, E., Velbel, M., and Krom, M. (1980) Dissolution of pyroxenes and amphiboles during weathering. *Science*, **207**, 1205–1206.

Berry, J.L. (1976) Study of chemical weathering in the Coweeta Hydrologic Laboratory, Macon County, North Carolina, 62 pp. Unpublished report.

Blum, A.E. and Lasaga, A.C. (1987) Monte Carlo simulations of surface reaction rate laws. Pp. 255–292 in: *Aquatic Surface Chemistry* (W. Stumm, editor). John Wiley & Sons, New York.

Blum, A.E. and Stillings, L.L. (1995) Feldspar dissolution kinetics. Pp. 291–342 in: *Chemical Weathering Rates of Silicate Minerals* (A.F. White and S.L. Brantley, editors). Reviews in Mineralogy **31**, Mineralogical Society of America, Washington, D.C.

Brantley, S.L. (2005) Reaction kinetics of primary rock-forming minerals under ambient conditions. Pp. 73–117

in: *Surface and Ground Water, Weathering, and Soils* (J.I. Drever, editor), Treatise on Geochemistry **5**, Elsevier-Pergamon, Oxford, UK.

Brantley, S.L. (2008) Kinetics of mineral dissolution. Pp. 151–210 in: *Kinetics of Water–Rock Interaction* (S.L. Brantley, J.D. Kubicki, and A.F. White, editors). Springer, New York.

Brantley, S.L. and Chen, Y. (1995) Chemical weathering rates of pyroxenes and amphiboles. Pp. 119–172 in: *Chemical Weathering Rates of Silicate Minerals* (A.F. White and S.L. Brantley, editors). Reviews in Mineralogy, **31**, Mineralogical Society of America, Washington, D.C.

Brantley, S.L., Crane, S.R., Crerar, D.A., Hellmann, R., and Stallard, R. (1986) Dissolution at dislocation etch pits in quartz. *Geochimica et Cosmochimica Acta*, **50**, 2349–2361.

Browning, S. and Thomas, D. (1985) Soil map of Coweeta Hydrologic Laboratory. U.S. Department of Agriculture, Forest Service, Southeastern Forest Experiment Station.

Bryan, D.S. (1994) Factors controlling the occurrence and distribution of hematite and goethite in soils and saprolites derived from schists and gneisses in western North Carolina. M.S. thesis, Michigan State University, East Lansing, Michigan, USA, 125 pp.

Campbell, A. and Schwertmann, U. (1984) Iron oxide mineralogy of placic horizons. *Journal of Soil Science*, **35**, 569–582.

Ciampone, M.A. (1995) Non-systematic weathering profile on metamorphic rock in the southern Blue Ridge Mountains, North Carolina: Petrography, bulk chemistry, and mineral chemistry of biotite. M.S. thesis, University of Cincinnati, Cincinnati, Ohio, USA, 86 pp.

Deer, W.A., Howie, R.A., and Zussman, J. (1997) *Rock-Forming Minerals – Orthosilicates*, **1A**, second edition. The Geological Society, London.

Drever, J.I. (1973) The preparation of oriented clay mineral specimens for X-ray diffraction analysis by a filter-membrane peel technique. *American Mineralogist*, **58**, 553–554.

Embrechts, J. and Stoops, G. (1982) Microscopical aspects of garnet weathering in a humid tropical environment. *Journal of Soil Science*, **33**, 535–545.

Fromhold, A.T., Jr. (1976) *Theory of Metal Oxidation. I. Fundamentals*. Defects in Crystalline Solids Series, **9**. North-Holland, Amsterdam.

Gardner, L.R. (1992) Long-term isovolumetric leaching of aluminum from rocks during weathering: Implications for the genesis of saprolite. *Catena*, **19**, 521–537.

Ghabru, S., Mermut, A., and St. Arnaud, R. (1989) Characterization of garnets in a typic Cryoboralf (Gray luvisol) from Saskatchewan, Canada. *Soil Science of America Journal*, **53**, 575–582.

Graham, R., Weed, S., Bowen, L., and Buol, S. (1989a) Weathering of iron-bearing minerals in soils and saprolite on the North Carolina Blue Ridge Front: I. Sand-size primary minerals. *Clays and Clay Minerals*, **37**, 19–28.

Graham, R., Weed, S., Bowen, L., and Buol, S. (1989b) Weathering of iron-bearing minerals in soils and saprolite of the North Carolina Blue Ridge Front: II. Clay Mineralogy. *Clays and Clay Minerals*, **37**, 29–40.

Graham, R., Daniels, R., and Buol, S. (1990a) Soil geomorphic relations on the Blue Ridge Front: I. Regolith types and slope processes. *Soil Science Society of America Journal*, **54**, 1362–1367.

Graham, R., Daniels, R., and Buol, S. (1990b) Soil geomorphic relations on the Blue Ridge Front: II. Soil Characteristics and Pedogenesis. *Soils Science Society of America Journal*, **54**, 1367–1377.

Hansley, P.L. (1987) Petrologic and experimental evidence for the etching of garnets by organic acids in the Upper Jurassic Morrison Formation, northwestern New Mexico. *Journal of Sedimentary Petrology*, **57**, 666–681.

Hatcher, R.D. (1980) Geologic map of Coweeta Hydrologic Laboratory, Prentiss Quadrangle, North Carolina: State of North Carolina, Department of Natural Resources and Community Development, in Cooperation with the Tennessee Valley Authority, scale 1:14,400, 1 sheet.

Hatcher, R.D. (1988) Bedrock geology and regional geologic setting of Coweeta Hydrologic Laboratory in the Eastern Blue Ridge. Pp. 81–92 in: *Forest Hydrology and Ecology at Coweeta* (W.T. Swank and D.A. Crossley, Jr., editors). Springer-Verlag, New York.

Hauffe, K. (1965) *Oxidation of Metals*. Plenum, New York.

Kretz, R. (1983) Symbols for rock-forming minerals. *American Mineralogist*, **68**, 277–279.

Klein, C. and Hurlbut, C.S. (1999) *Manual of Mineralogy*. John Wiley & Sons, Inc., New York.

Kubaschewski, O. and Hopkins, B.E. (1962) *Oxidation of Metals and Alloys* (2nd edition). Butterworths, London.

Lasaga, A. and Blum, A. (1986) Surface chemistry, etch pits and mineral water reactions. *Geochimica et Cosmochimica Acta*, **50**, 2363–2379.

Lüttge, A. and Arvidson, R.S. (2008) The mineral–water interface. Pp. 73–107 in: *Kinetics of Water–Rock Interaction* (S.L. Brantley, J.D. Kubicki, and A.F. White, editors). Springer, New York.

Miller, C.F., Hatcher, R.D., Jr., Ayers, J.C., Coath, C.D., and Harrison, T.M. (2000) Age and zircon inheritance of eastern Blue Ridge plutons, southwestern North Carolina and northeastern Georgia, with implications for magma history and evolution of the southern Appalachian orogen. *American Journal of Science*, **300**, 142–172.

Moore, D.M. and Reynolds, Jr., R.C. (1997) X-*ray Diffraction and the Identification and Analysis of Clay Minerals*. Oxford University Press, New York.

Parisot, J.C., Delvigne, J., and Groke, M.T.C. (1983) Petrographical aspects of the supergene weathering of garnet in the Serra dos Carajas (Para, Brazil). P. 47 in: *International Colloquium CNRS on the Petrology of Weathering and Soils, Abstracts* (D. Nahon and Y. Noack, editors). Centre National de la Recherche Scientifique, Paris.

Price, J.R. (2003) Allanite weathering and rare earth elements in mass balance calculations of clay genesis rates at the Coweeta Hydrologic Laboratory, western North Carolina, USA: The response times of changes in clay mineral assemblages to fluctuations in climate. Ph.D. thesis, Michigan State University, East Lansing , Michigan, USA, 237 pp.

Price, J.R., Velbel, M.A., and Patino, L.C. (2005) Rates and timescales of clay-mineral formation in the southern Appalachian Mountains from geochemical mass balance, *Geological Society of America Bulletin*, 117, 783–794.

Robertson, I.D.M. and Butt, C.R.M. (1997) *Atlas of Weathered Rocks*. CRC LEME Open File Report **390**, 1st Revision. Cooperative Research Centre for Landscape Evolution and Mineral Exploration, Wembley, Western Australia.

Salvino, J.F. and Velbel, M.A. (1989) Faceted garnets from sandstones of the Munising Formation (Cambrian), northern Michigan: petrographic evidence for origin by intrastratal dissolution. *Sedimentology*, **36**, 371–379.

Schott, J. and Petit, J.-C. (1987) New evidence for the mechanisms of dissolution of silicate minerals. Pp. 255–292 in: *Aquatic Surface Chemistry* (W. Stumm, editor). John Wiley & Sons, New York.

Schroeder, P.A., Melear, N.D., West. L.T., and Hamilton, D.A. (2000) Meta-gabbro weathering in the Georgia Piedmont, USA: implications for global silicate weathering rates. *Chemical Geology*, **163**, 235–245.

Schwertmann, U. (1971) Transformations of hematite to goethite in soils. *Nature*, **232**, 624–625.

Smyth, J.R. and Bish, D.L. (1988) *Crystal Structures and Cation Sites of the Rock-Forming Minerals*. Allen & Unwin, Boston, Massachusetts, USA.

Swank, W. and Crossley, I. (1988) Introduction and site description. Pp. 3–15 in: *Forest Hydrology and Ecology at Coweeta* (W.T. Swank and D.A. Crossley, Jr., editors). Springer-Verlag, New York.

Velbel, M. (1984a) Natural weathering mechanisms of almandine garnet. *Geology*, **12**, 631–634.

Velbel, M. (1984b) Mineral transformations during rock weathering, and geochemical mass-balances in forested watersheds of the Southern Appalachians. Ph.D. thesis, Yale University, New Haven, Connecticut, USA, 175 pp.

Velbel, M. (1985) Geochemical mass balances and weathering rates in forested watersheds of the southern Blue Ridge. *American Journal of Science*, **285**, 904–930.

Velbel, M.A. (1988) Weathering and soil-forming processes, Pp. 93–102 in: *Forest Hydrology and Ecology at Coweeta* (W.T. Swank and D.A. Crossley, Jr., editors). Springer-Verlag, New York.

Velbel, M.A. (1989) Weathering of hornblende to ferruginous products by a dissolution-reprecipitation mechanism: petrography and stoichiometry. *Clays and Clay Minerals*, **37**, 515–524.

Velbel, M.A. (1990) Mechanisms of saprolitization, isovolumetric weathering, and pseudomorphous replacement during rock weathering – a review. *Chemical Geology*, **84**, 17–18.

Velbel, M.A. (1993) Formation of protective surface layers during silicate-mineral weathering under well-leached, oxidizing conditions. *American Mineralogist*, **78**, 408–417.

Velbel, M.A. (2004) Laboratory and homework exercises in the geochemical kinetics of mineral–water reaction: rate law, Arrhenius activation energy, and the rate-determining step in the dissolution of halite. *Journal of Geoscience Education*, **52**, 52–59.

Velbel, M.A. (2007) Surface textures and dissolution processes of heavy minerals in the sedimentary cycle: examples from pyroxenes and amphiboles. Pp. 113–150 in: *Heavy Minerals in Use* (M.A. Mange and D.T. Wright, editors). Developments in Sedimentology, **58**, Elsevier, New York.

Velbel, M.A. and Barker, W.W. (2008) Pyroxene weathering to smectite: Conventional and low-voltage cryo-field emission scanning electron microscopy, Koua Bocca ultramafic complex, Ivory Coast. *Clays and Clay Minerals*, **56**, 111–126.

Velbel, M.A., McGuire, J.T., and Madden, A.S. (2007) Scanning electron microscopy of garnet from southern Michigan soils: Etching rates and inheritance of pre-glacial and pre-pedogenic grain-surface textures. Pp. 413–432 in: *Heavy Minerals in Use* (M.A. Mange and D.T. Wright, editors). Developments in Sedimentology, **58**, Elsevier, New York.

Velbel, M.A., Donatelle, A.R., and Formolo, M.J. (2009) Reactant-product textures, volume relations, and implication for major-element mobility during natural weathering of hornblende, Tallulah Falls Formation, Georgia Blue Ridge, U.S.A. *American Journal of Science*, **309**, 661–688.

Wendt, A., D'Arco, P., Goffé, B., and Oberhänsli, R. (1993) Radial cracks around α-quartz inclusions in almandine: Constraints on the metamorphic history of the Oman Mountains. *Earth and Planetary Science Letters*, **114**, 449–461.

White, A.F., Blum, A.E., Schulz, M.S., Vivit, D.V., Stonestrom, D.A., Larsen, M., Murphy, S.F., and Eberl, D. (1998) Chemical weathering in a tropical watershed, Luquillo Mountains, Puerto Rico: I. Long-term versus short-term weathering fluxes. *Geochimica et Cosmochimica Acta*, **62**, 209–226.

Wilson, M.J. (1975) Chemical weathering of some primary rock-forming minerals. *Soil Science*, **119**, 349–355.

Yeakley, J.A., Swank, W.T., Swift, L.W., Hornberger, G.M., and Shugart, H.H. (1998) Soil moisture gradients and controls on a southern Appalachian hillslope from drought through recharge. *Hydrology and Earth System Sciences*, **2**, 41–49.

(*Received 27 August 2012; revised 18 February 2013; Ms. 706; AE: W.D. Huff*)